



BENG INDIVIDUAL PROJECT

IMPERIAL COLLEGE LONDON

DEPARTMENT OF COMPUTING

Emulating the Quantum Valley Hall Effect in Topologically Perturbed Model Systems

Author:
Bernard Ting

Supervisor:
Prof. Richard Craster

Second Marker:
Dr. Christopher Ford

June 19, 2019

Abstract

We investigate how the topological perturbation of an elastic mass-spring system leads to the formation of bandgaps which behave similarly to the quantum valley-Hall effect. We first introduce the theory of dispersion curves and plot them for simple models. We then break the symmetry by introducing masses of different weights and observe induces a bandgap. The resulting structures composed of two media with different topological invariants have non-trivial bandgaps which support edge waves at the interface. We analyse the dispersion relations on the unit cell and finite strip to find special frequencies or modes which are present in the band gap. Numerical scattering simulations are then run with these frequencies induced to the lattice to confirm our analysis. This work proposes several different ways of topologically perturbing lattices as well as seek to show that this simple model is able to emulate the behaviours and effects seen in more complex systems.

Acknowledgements

I would like to extend my greatest thanks to my supervisor, Prof. Richard Craster, for his advice and guidance on all matters relating to the project. I would also like to thank Dr. Christopher Ford for being my second marker and providing timely feedback regarding my project.

Contents

1	Introduction	3
1.1	Objectives	3
1.2	Motivation	3
2	Background	4
2.1	History	4
2.2	Practical applications	4
2.3	Models studied	5
2.4	Dispersion relation	7
2.5	Bloch waves	7
2.6	Reciprocal lattice	7
2.7	Brillouin zone	8
3	Dispersion relation	10
3.1	1d lattice	10
3.2	2d square lattice	12
3.3	2d hexagonal lattice	15
3.4	2d kagome lattice	18
4	Perturbed system	23
4.1	Band gap	23
4.2	2d bulk hexagonal perturbation	24
4.2.1	Alternating masses	24
4.2.2	Varying mass and stiffnesses	24
4.3	2d hexagonal strip	25
4.3.1	Alternating masses	28
4.3.2	Varying mass and stiffnesses	30
4.4	2d bulk kagome perturbation	30
4.5	2d kagome strip	31
5	Scattering simulation	35
5.1	Our linear system in physical space	35
5.2	2d hexagonal finite lattice	35
5.2.1	Alternating masses	36
5.2.2	Varying mass and stiffnesses	38
5.3	2d kagome finite lattice	38
6	Complex bends	41
6.1	Gentle and sharp straight bends	41
6.2	Curved bends	41
6.3	Energy splitting and merging	41
7	Evaluation	46
7.1	Reproducibility in other models	46
7.2	Extensibility and reusability of codebase	46
7.3	Further work	48
8	Conclusion	51

Chapter 1

Introduction

Many advances in the realm of photonics, phononics and even next-generation electronics come from the ability to manipulate and control wave energy.¹⁻⁸ Most of technologies depend on being able to direct wave propagation as well as split and merge waves on demand without loss of energy. Many recent advances have come from the application of topological concepts to guided wave propagation.⁹⁻¹² One such phenomenon is the quantum valley-Hall effect which exploits valley states to achieve topologically protected edge modes in a lattice of electrons by creating time-reversal symmetric valley-Hall insulators,¹³⁻¹⁵ which can be used to direct wave propagation. Hence in this work, we will be investigating 2-dimensional mass-spring systems that emulate the quantum valley-Hall effect. This provides the ability to experiment, explore and simulate other novel behaviours and properties in a simpler system. Though we do not break time reversal symmetry in our model (i.e. we have two way propagation), we break the physical symmetry of our lattices to get as close as we can to their effects.

1.1 Objectives

In this project, our main goal is to emulate the quantum valley Hall effect^{11, 16} in a model mass-spring system. We will then use these systems to geometrically navigate waves around different bends by constructing a finite lattice composed of two topologically different materials where the elastic waves will travel along the boundary between the two materials.

In particular, we will be carrying out the following:

1. Build an intuition to study dispersion relations by first finding them for simpler models. (Chapter 3)
2. Perturb structures of elementary cells of infinite lattices to open up band gaps. Then construct a semi-infinite lattice formed of ribbons created from two differently perturbed elementary cells and observe wave behaviour at the boundary. (Chapter 4)
3. Simulate scattering to confirm direction of dissipation of energy. (Chapter 5)

Though the construction and fabrication of metamaterials involve much more considerations in terms of material science, in our case, we are experimenting on toy model systems computationally to discover new properties and behaviours. This will allow us to investigate new phenomena in the context of a much simpler system. And if we are able to experimentally verify the observations we see in our simulations as well as corroborate results found in other more complex models, we can then go on to perform more interesting further work on this toy model.

1.2 Motivation

There are many reasons to want to create metamaterials which can control the directions of electromagnetic or acoustic waves. As we discuss in Chapter 2.2, metamaterials have the capability to solve many engineering problems. However, metamaterials manufacturing presents many challenges including requiring machines which are capable of reliably working on the micro- and nano-scale.¹⁷ Therefore, being able to model and investigate their properties computationally will allow us to decrease prototyping time as well as discover new features which might be of interest efficiently.

Chapter 2

Background

Waves exhibit many characteristics when travelling through different media. Much research has been carried out to investigate and harness these properties to develop technologies and devices which manipulate electromagnetic (photonic) and also acoustic (phononic) waves.

2.1 History

Since the earliest days of human history, we have sought to better understand the natural world around us and so create technologies to improve our lives. At first by utilising what nature already has to offer, but later on developing materials and devices which have desirable properties not found in nature.

This progression describes roughly how the study of metamaterials came about. It began in 1887 with the study of how certain crystals exhibit interesting iridescence.¹⁸ After two independently developed landmark papers were published in 1987 on structures with band gaps for electromagnetic waves,^{19,20} the term photonic crystal — a periodic optical nanostructure which manipulates the passage of electromagnetic radiation — was coined.²¹ Since then, photonic crystals have been mass produced and used for many purposes, e.g. optical fibres for transmission of digital information²² and precision surgery.^{23,24}

Then came the study of metamaterials — materials engineered to possess some property not found in naturally occurring materials.²⁵ Usually these materials are composed of smaller units which are arranged in a repeating pattern. They derive their properties not from the intrinsic properties of the base materials, but from the periodic structure introduced.

One of the first major breakthroughs which the study of metamaterials led to was the development of materials with a negative refractive index. Though the possibility of creating such a material was theoretically predicted in 1967,²⁶ it was only experimentally verified in 2001.²⁷

Nowadays, there is much research being done in the area of topological metamaterials or topological photonic crystals.^{7,28,29} This is where new properties of metamaterials are produced by perturbing their structures utilising topological and group theoretic concepts, usually by breaking symmetries which are present in the original material. The reason there is considerable interest in applying these abstract fields to the study of metamaterials is due to their ability to transcend specific physical systems and be applied widely. An example is being able to create metamaterials which split energy in multiple directions.⁷ Since then, much research has been done in emulating these topological effects in simpler systems and then transferring the results into proper experimentation in the desired contexts.^{9,30-32} This forms an exciting modern area of wave physics and we mention below some of the novel applications which can be realised with these systems.

2.2 Practical applications

Metamaterials have the potential to solve many modern engineering problems. Some of which are mentioned below:

- Developing a cloak of invisibility.²
 - Obvious use cases in military.

- Protect things from electromagnetic radiation.
- Constructing antennae to focus energy into narrow beams.^{3,4}
 - Gather wave energy from deep in the oceans and concentrate them to be harvested.
 - Channel sound energy, e.g. from train tracks, to be dissipated elsewhere which decreases noise pollution.
- Producing devices which operate on the terahertz ($1\text{THz} = 10^{12}\text{Hz}$) range.⁵
 - Can be used in medical imaging due to terahertz radiation being able to penetrate thin materials but not thicker objects. Also, it is non-ionising radiation and so does not damage living cells unlike X-rays.
 - For surveillance, especially security screening as many materials of interest have unique spectral fingerprints in the THz range.³³
- Developing near perfect electromagnetic absorbers.⁶
- Developing energy splitters.⁷
- Developing perfect lenses.⁸

2.3 Models studied

There are many different models which we can use to study the effects of metamaterials on the waves which propagate through them.

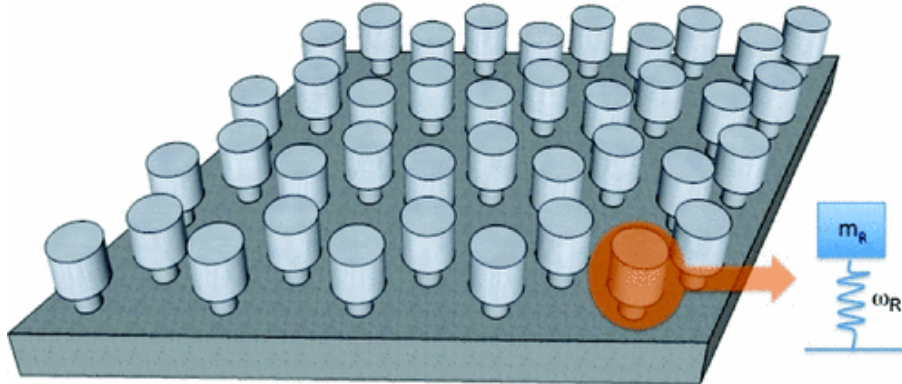


Figure 2.1: Schematic view of a thin plate flexural wave model which consists of an array of resonators attached to a thin elastic plate. Each resonator is a point mass attached to the plate by a spring. Image adapted from source.³⁴

In the literature, thin plate flexural wave theories,^{35,36} as seen in Figure 2.1, have proven to be highly effective physical models and reliable predictors of physical wave phenomena as shown by the numerous studies done on flexural (or bending) waves in a beam or a plate.^{34,37,38} This is very advantageous as most acoustic (or sound) radiation travels as flexural waves through structures and deforms the medium transversely as they propagate.³⁹ Therefore, these models are very useful in studying acoustic metamaterials or phononic crystals.⁴⁰ As a specific example, an elastic analogue of graphene, a honeycomb arrangement of mass-spring resonators attached to a thin elastic plate, was shown which could be used as waveguides.³⁴

Having said that, the equations which govern the propagation of flexural waves are much more complicated than those for a simple mass-spring system and requires more background knowledge in its physics to properly understand and implement. As an example, the biharmonic equation which governs the propagation of flexural waves in a lattice of mass-spring resonators is a fourth-order partial differential equation.

Along the same lines, the modelling of electromagnetic metamaterials present the challenges of getting to grips with the theory of electromagnetic radiation, e.g. Maxwell's equations⁴¹ and Bragg scattering.⁴²

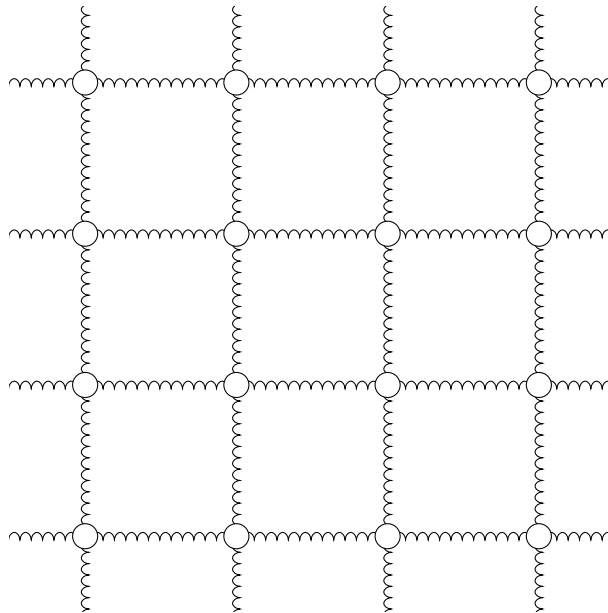


Figure 2.2: Schematic view of our simple mass-spring model.

Given the timeline of this project, the limited Physics background I have, as well as to make the results accessible to a wider audience, we have decided to go for a simplistic masses-connected-by-springs model, as seen in Figure 2.2, as the core object of study in our project. The lattice will be formed of repeating cells (e.g. Figure 3.3) and it is the periodicity in the lattice which will give rise to its special properties. Not only does this reduce the complexity as we only need to deal with ordinary differential equations and not partial differential equations, it also reduces the complexity in the scattering simulations as we now have to solve a discrete system instead of a continuous one. With this *toy* system which form the basic building blocks of solid state physics, we will be able to more quickly lay the foundations required to carry out more interesting experiments, from which results can be transferred to other models.

The two lattices which we will be focusing most of this work on is the hexagonal and kagome lattice. This is because they have a lot of physical analogues which are particularly useful.^{9, 43, 44} As a concrete example, the kagome lattice shown in Figure 3.13 has a physical analogue as a dense packed system such as the one shown in Figure 2.3. The dense packed system consists of particles and voids filled with fluid connected by thin gaps and is a good representation for certain photonic and phononic crystals. The key to controlling the behaviour of the crystal is being able to precisely engineer the thin gaps, as the gaps and voids together form a connected network of resonators.⁴⁴ Thus, it can be seen that our model is asymptotically equivalent to this physical system.⁴⁴

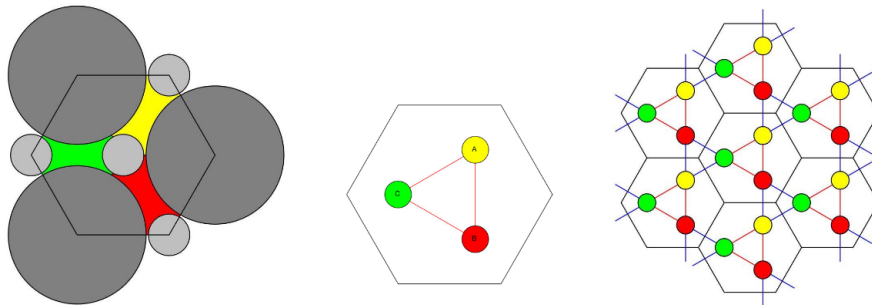


Figure 2.3: The closely packed system (left) shows rigid cylindrical inclusions of two different radii, the elementary hexagonal cell and the three voids (yellow, green, red) connected by thin gaps. The asymptotically equivalent Kagome lattice as a discrete network model (right). Image and caption adapted from source.⁴⁴

The following will be brief explanations of concepts which will form the foundation on which

we will analyse and investigate the properties of our lattices.

2.4 Dispersion relation

A dispersion relation relates the wavenumber of a wave to its frequency. We will see that this relation is of utmost importance when discussing periodic lattices as only waves of certain frequencies are transmitted by the lattice and the dispersion relation directly shows us which frequencies these are. As we will be solving for the dispersion relation of infinite and semi-infinite lattices in Chapter 3 and 4, we will be making use of the concepts below to simplify the problem (because we do not want to solve an infinite problem!).

2.5 Bloch waves

Bloch's theorem for waves in a periodic potential⁴⁵ states that any wave travelling through a periodic potential can be expressed as the product of a periodic function and a plane wave,⁴⁶ i.e.

$$\psi_{\vec{\kappa}}(\vec{r}) = f_{\vec{\kappa}}(\vec{r})e^{i\vec{\kappa}\cdot\vec{r}} \quad (2.1)$$

where $f_{\vec{\kappa}}(\vec{r})$ has the period of the lattice with $f_{\vec{\kappa}}(\vec{r}) = f_{\vec{\kappa}}(\vec{r} + \vec{R})$, with \vec{R} being a translation vector of the lattice.

The proof of this theorem can be found here.⁴⁶ But we will just state how we can use this result to simplify the equations we will obtain in our systems. This is useful for us as we are modelling elastic waves travelling through a periodically-repeating mass-spring system and so Bloch's theorem applies. Thus we can write the displacement of one mass as the displacement of another *corresponding* mass in the lattice multiplied by a complex exponential factor. By doing this, we can characterise the behaviour of all the displacements by just focusing on finding the displacements of masses in the *primitive cell*, which is just the unit cell which forms the repeating base of our lattice. We will see later how this helps to reduce our infinite system of equations down to a finite number, such as in (3.7) and (3.12).

2.6 Reciprocal lattice

A reciprocal lattice represents the Fourier transform of another lattice. In our case, our model lattice is a periodic spatial function in real space, and so its reciprocal lattice exists as a function of frequency in reciprocal space. We will continue with a more formal explanation based on the materials in the Appendix of this book,⁴⁷ restricting our discussion to only 2-dimensional lattices which is sufficient for our purposes.

More formally, suppose we have a function $f(\vec{r})$ which is periodic on a lattice, i.e. $f(\vec{r}) = f(\vec{r} + \vec{R})$ for all vectors \vec{R} that translate the lattice onto itself (connect a lattice point to the next). Then we call \vec{R} the *lattice vectors*. As we shall see later, elastic waves travelling through our mass-spring lattices are examples of such a periodic function. Naturally then, we would take the Fourier transform when analysing a periodic function, i.e.

$$f(\vec{r}) = \int c\vec{q}g(\vec{q})e^{i\vec{q}\cdot\vec{r}} \quad (2.2)$$

Applying periodicity, we see that

$$f(\vec{r} + \vec{R}) = f(\vec{r}) \quad (2.3)$$

$$\Rightarrow \int c\vec{q}g(\vec{q})e^{i\vec{q}\cdot\vec{r}}e^{i\vec{q}\cdot\vec{R}} = \int c\vec{q}g(\vec{q})e^{i\vec{q}\cdot\vec{r}} \quad (2.4)$$

$$\Rightarrow g(\vec{q}) = g(\vec{q})e^{i\vec{q}\cdot\vec{R}} \quad (2.5)$$

Therefore, this tells us that the transform $g(\vec{q})$ has to be zero everywhere, except where $e^{i\vec{q}\cdot\vec{R}} = 1$, or equivalently $\vec{q}\cdot\vec{R} = 2\pi N$ for any $N \in \mathbb{Z}$. These vectors \vec{q} that satisfy this condition are called

the *reciprocal lattice vectors* and are usually designated by \vec{G} . Note also that these reciprocal lattice vectors form a lattice of their own, which we can easily verify as

$$(\vec{G}_1 + \vec{G}_2) \cdot \vec{R} = \vec{G}_1 \cdot \vec{R} + \vec{G}_2 \cdot \vec{R} = 2\pi(N_1 + N_2) \quad (2.6)$$

and we call this reciprocal lattice the *reciprocal space*.

So given a set of lattice vectors \vec{R} , to find the reciprocal lattice vectors \vec{G} , we need to find all \vec{G} such that $\vec{G} \cdot \vec{R}$ is some integer multiple of 2π for every \vec{R} . Since we know that $\{\vec{G}\}$ forms a lattice, we know that every reciprocal lattice vector \vec{G} can be written as $\vec{G} = l\vec{b}_1 + m\vec{b}_2$ for some set of primitive lattice vectors \vec{b}_i , similar to how any lattice vector \vec{R} can be written as $\vec{R} = p\vec{a}_1 + q\vec{a}_2$ for some set of primitive lattice vectors \vec{a}_i which are the smallest vectors pointing from one lattice point to another and need not be of unit length. Therefore

$$\vec{G} \cdot \vec{R} = 2\pi N \quad (2.7)$$

$$\Rightarrow (p\vec{a}_1 + q\vec{a}_2) \cdot (l\vec{b}_1 + m\vec{b}_2) = 2\pi N \quad (2.8)$$

From this, it is easy to see that constructing \vec{b}_i such that $\vec{a}_i \cdot \vec{b}_j = 2\pi\delta_{ij}$ satisfies the above condition. Therefore we see from this that if \vec{a}_i is of length a , then \vec{b}_i will be of length $\frac{2\pi}{a}$, which is where the term *reciprocal* lattice is derived from.

2.7 Brillouin zone

The concept of Brillouin zones was first defined by Leon Brillouin in his book on wave propagation in periodic structures.⁴⁸ As we are able to tessellate our physical lattice with a periodically repeating unit cell, so there exists a unit reciprocal cell which can cover the reciprocal space without overlap. We will now motivate the selection of the first Brillouin zone as a *good* unit reciprocal cell based on the discussions in here.⁴⁷

To see how we might make a good choice for a unit cell for the reciprocal space, notice that for the Bloch states (as defined in Chapter 2.5), different values of $\vec{\kappa}$ do not necessarily lead to different modes. To be more precise, the modes with wave vector $\vec{\kappa}$ and $\vec{\kappa} + 2\pi\vec{N}$ are identical, which means that $\vec{\kappa}$ essentially functions as the phase relationship between the displacement of masses in our lattice. Now notice also that from (2.1) and the fact that our lattice is periodic, we have that if \vec{G} is a reciprocal lattice vector (as defined in Chapter 2.6), then $\vec{\kappa} + \vec{G}$ causes the phase difference between masses to be incremented by $\vec{G} \cdot \vec{R}$ which we know is $2\pi N$ and so is no difference at all!

This shows us that there is a lot of redundancy in $\vec{\kappa}$ and we do not actually need to explore the whole of κ -space but it is enough for us to restrict ourselves to a finite *zone* in the reciprocal space from which we *cannot* get from one part of the lattice to another by adding \vec{G} . This is visually demonstrated in Figure 2.4.

There are many such zones, but we choose to focus on the region which is closest to the origin, where $\vec{\kappa} = 0$. And that zone is what we call the first Brillouin zone.

That is why the other way to define a Brillouin zone is that it is a particular choice of this reciprocal cell and is constructed as the set of points enclosed by the Bragg planes. The Bragg planes exist in reciprocal space and are the planes perpendicular to a straight line from the origin to each lattice point. The first Brillouin zone is then defined as the set of points formed by the Bragg planes closest to the origin. These concepts are described visually for a 2d square real lattice in Figure 3.4.

The idea of Brillouin zones is brilliant in that now we know we only need to solve for the dispersion relation for $\vec{\kappa}$ in the first Brillouin zone to know the dispersion relation across the entire lattice.

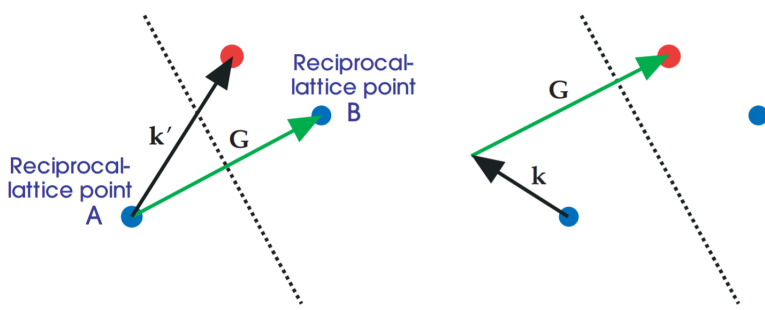


Figure 2.4: Characterisation of the Brillouin zone. The dotted line refers to the perpendicular bisector of the line joining two reciprocal lattice points (blue). Notice that if we choose the left point A as the origin, any lattice vector (such as $\vec{\kappa}'$) that reaches to an arbitrary point on the other side (red) can be expressed as the sum of a vector on the same side (such as $\vec{\kappa}$) plus a reciprocal lattice vector \vec{G} . Image and caption adapted from source.⁴⁷

Chapter 3

Dispersion relation

As mentioned in Chapter 2.4, the dispersion relation succinctly characterises a given periodic lattice. As such, we will start with discussing how we can find the dispersion relations for simple lattices.

3.1 1d lattice

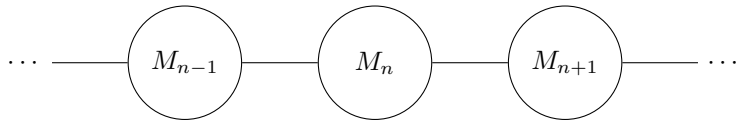


Figure 3.1: Schematic view of our 1d model.

Let us start our discussion with the most basic one-dimensional case. In this case, we have masses of equal mass, m spread out evenly across one dimension. All neighbouring masses are connected by an elastic force which scales proportionally with distance, i.e. $F = kx$ for some k .

Note: As mentioned before, we will be thinking of this system as a mass-spring system. Notice however that it does not matter whether we are considering longitudinal or transverse waves, as the equations governing their interactions are the same. In our discussions, we will be considering the waves propagating through our models as transverse waves. This helps to simplify visualisations as the displacements and movements of the masses are perpendicular to the lattice on which they are bound.

With this one-dimensional case set up, we now want to find out what forms of waves it allows to propagate. We do this by considering only nearest neighbour interactions and examining the elementary unit of the lattice which can be repeated by translation to form the full lattice.

So let us consider three masses side-by-side in our lattice, M_{n-1} , M_n and M_{n+1} which are y_{n-1} , y_n and y_{n+1} displacement away from their equilibrium positions. By focusing on the centre mass and considering only nearest neighbour interactions, by Hooke's Law, we have that the force on M_n

$$F_n = \sum F = k(y_{n-1} + y_{n+1} - 2y_n) \quad (3.1)$$

At the same time, we have by Newton's 2nd Law that

$$F_n = m \frac{d^2}{dt^2} y_n \quad (3.2)$$

Taking y_n to be the general wave solution

$$y_n = \hat{y}_n e^{-i\Omega t} \quad (3.3)$$

$$\Rightarrow \frac{d^2}{dt^2} y_n = -\Omega^2 y_n \quad (3.4)$$

$$\Rightarrow F_n = -m\Omega^2 y_n \quad (3.5)$$

where Ω is the frequency of the wave and \hat{y}_n is the complex amplitude.

Therefore, we have by (3.1) and (3.5) that

$$-m\Omega^2 y_n = k(y_{n-1} + y_{n+1} - 2y_n) \quad (3.6)$$

$$\Rightarrow \left(-\frac{m}{k}\Omega^2 + 2\right)y_n - y_{n-1} - y_{n+1} = 0 \quad (3.7)$$

Since we can write this differential equation for any of our masses in our infinite lattice, we would need to solve an infinite number of coupled second order differential equations. However, the trick we use is that since we have that M_{n-1} and M_{n+1} are equidistant from M_n at equilibrium (i.e. the lattice is periodic), we can make use of Bloch's theorem (discussed in Chapter 2.5 to describe the phase shift in the wave solution as

$$y_{n-1} = e^{-i\kappa} y_n, \quad y_{n+1} = e^{i\kappa} y_n \quad (3.8)$$

Hence, from (3.7), we see that

$$\left(-\frac{m}{k}\Omega^2 + 2 - e^{-i\kappa} - e^{i\kappa}\right)y_n = 0 \quad (3.9)$$

$$\Rightarrow \cos(\kappa) = -\frac{m}{2k}\Omega^2 + 1 \quad (3.10)$$

Therefore, we now have an equation linking the wave number κ and the frequency Ω of waves propagating across our 1d lattice. By initialising m and k we can use this equation to plot the dispersion curve of our system. By setting $m = k = 1$, we get the dispersion curve in Figure 3.2.

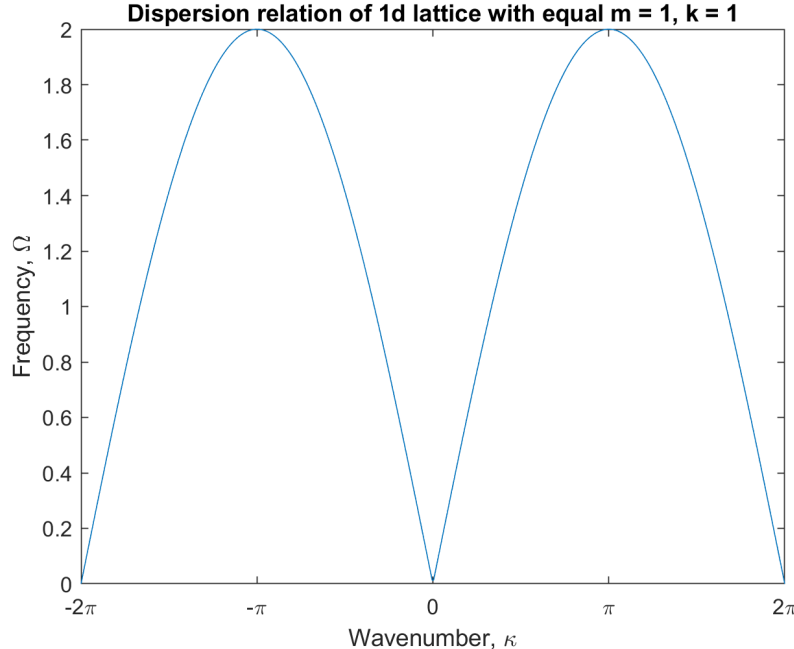


Figure 3.2: Dispersion relation of a 1d monoatomic chain.

The first interesting thing to notice about this dispersion relation is that the curve seems to be periodically repeating. More precisely, if we look at the curve between $-\pi$ and π , we can see

that translating this portion of the graph left or right by 2π will give us the rest of the dispersion relation. This range of wave numbers is known as the first Brillouin zone, which we discuss more in the context of 2d lattices in Chapter 2.7.

3.2 2d square lattice

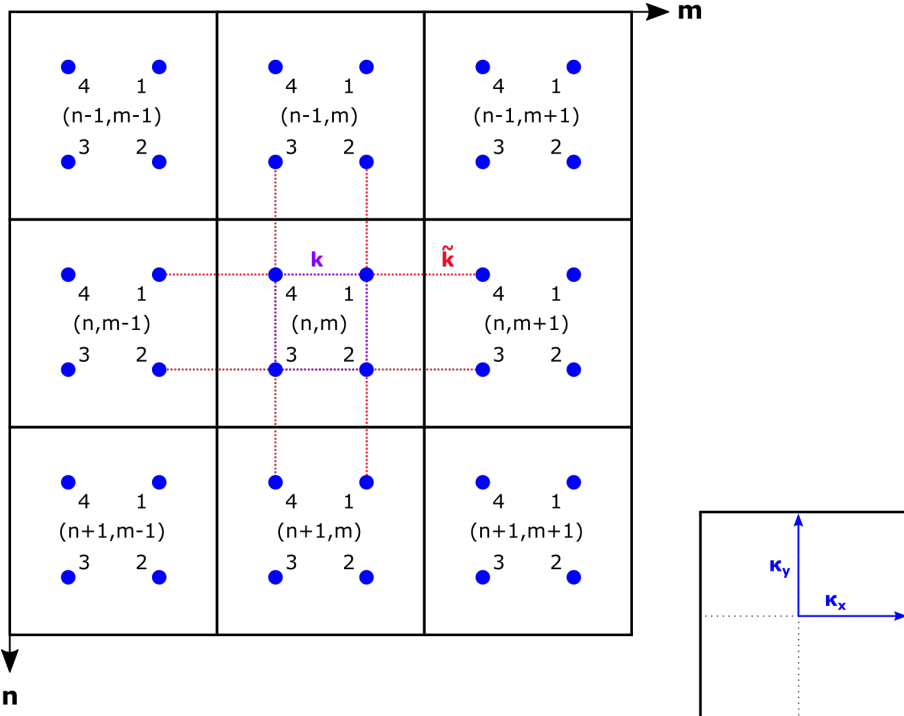


Figure 3.3: Schematic view of our 2d model. Each square tile in the grid corresponds to one elementary cell with four masses. k and \tilde{k} represent the intra- and inter-cell spring constants respectively. The cell in the far bottom right shows the directions of the Bloch phases. Note that only the elastic interactions involving the masses in cell (n, m) are shown to avoid cluttering the figure, although they exist within and between each cell.

We now extend this analysis to an infinite two-dimensional square lattice, as described in Figure 3.3. Each elementary square cell contains four masses M_i for $i \in [1, 4]$ which are arranged clockwise from the top right. We take n and m to be the vertical and horizontal directions respectively, with n increasing downwards and m increasing to the right, so that relative to cell (n, m) we have cell $(n - 1, m)$ above and cell $(n, m + 1)$ to the right. We have decided to go with this convention as it reflects matrix indexing in Matlab, which will simplify our code. With this setup, we can now label each mass and its displacement uniquely, e.g. M_i in cell (n, m) is labelled $M_i^{n,m}$ and has displacement $y_i^{n,m}$.

Note: Though we use this system to refer to specific masses in specific cells, the mass of each mass is determined solely by its position in its cell, i.e. $\forall n, m \in \mathbb{Z}$, the mass of $M_i^{n,m} = M_i$.

Each mass is elastically connected to its direct neighbours, e.g. $M_1^{n,m}$ is connected to $M_2^{n,m}$, $M_4^{n,m}$, $M_2^{n-1,m}$ and $M_4^{n,m+1}$. We have the spring constant k between masses in the same cell and \tilde{k} between masses in adjacent cells.

Now again we consider only nearest neighbour interactions. Focusing on the elementary cell (n, m) and its adjacent cells, using Hooke's law and Newton's 2nd law on each of the masses in cell (n, m) , we can get a second order differential equation which is coupled to the displacements of the other masses it is connected to. For example, considering $M_1^{n,m}$, we get

$$F_1 = M_1 \frac{d^2}{dt^2} y_1^{n,m} = k(y_2^{n,m} + y_4^{n,m} - 2y_1^{n,m}) + \tilde{k}(y_2^{n-1,m} + y_4^{n,m+1} - 2y_1^{n,m}) \quad (3.11)$$

Since we can write this differential equation for any of our masses in our infinite lattice, we would get an infinite number of coupled second order differential equation. However, similar to the 1d case, using the periodicity of the lattice and Bloch's theorem once more, we can relate the displacements of each mass to the corresponding mass in a *base cell* with the lattice vectors κ_y and κ_x , i.e.

$$y_i^{n+N, m+M} = e^{i(N\kappa_y + M\kappa_x)} y_i^{n, m} \quad \forall N, M \in \mathbb{Z} \quad (3.12)$$

With this, instead of an infinite number of equations, we have a set of four coupled second order differential equations, one for each $y_i^{n, m}$ for $i \in [1, 4]$. We now drop the superscripts (n, m) and assume we have a wave solution of the form

$$y_i = \hat{y}_i e^{-i\Omega t} \quad (3.13)$$

$$\Rightarrow \frac{d^2}{dt^2} y_i = -\Omega^2 y_i \quad (3.14)$$

$$\Rightarrow F_i = -M_i \Omega_i^2 y_i \quad (3.15)$$

where Ω is the frequency of the wave and \hat{y}_i is the complex amplitude. We can now rewrite (3.11) as

$$M_1 \Omega_1^2 y_1 = k(2y_1 - y_2 - y_4) + \tilde{k}(2y_1 - y_2 e^{-i\kappa_y} - y_4 e^{i\kappa_x}) \quad (3.16)$$

$$= (2k + 2\tilde{k}) y_1 + (-k - \tilde{k} e^{-i\kappa_y}) y_2 + (-k - \tilde{k} e^{i\kappa_x}) y_4 \quad (3.17)$$

By constructing this equation for each y_i , we can reformulate these four difference equations as an eigenvalue problem

$$[\mathbf{A}(\kappa_x, \kappa_y) - \boldsymbol{\Omega}\mathbf{M}] \vec{y} = \vec{0} \quad (3.18)$$

where $\boldsymbol{\Omega} = \text{diag}(\{\Omega_i^2\})$, $\mathbf{M} = \text{diag}(\{M_i\})$, $\vec{y} = [\{y_i\}]^T$ and

$$\mathbf{A}(\kappa_x, \kappa_y) = \begin{bmatrix} 2k + 2\tilde{k} & -k - \tilde{k} e^{-i\kappa_y} & 0 & -k - \tilde{k} e^{i\kappa_x} \\ -k - \tilde{k} e^{i\kappa_y} & 2k + 2\tilde{k} & -k - \tilde{k} e^{i\kappa_x} & 0 \\ 0 & -k - \tilde{k} e^{-i\kappa_x} & 2k + 2\tilde{k} & -k - \tilde{k} e^{i\kappa_y} \\ -k - \tilde{k} e^{-i\kappa_x} & 0 & -k - \tilde{k} e^{-i\kappa_y} & 2k + 2\tilde{k} \end{bmatrix} \quad (3.19)$$

Therefore, we can solve for the eigenvalues and eigenvectors of this equation. The eigenvalues of this equation correspond to the frequency of waves, Ω , which are allowed through our lattice while the eigenvectors correspond to the displacement of the masses, y_i . It is also interesting to note that because \mathbf{A} is Hermitian, we are guaranteed by the spectral theorem for Hermitian matrices that all the eigenvalues are real. However, the next question arises: How should we vary κ so that we get a good enough picture of the full dispersion relation of our 2d lattice?

To answer this question, we make use of the theory of Brillouin zones as discussed in Chapter 2.7 to form the first Brillouin zone for our infinite square lattice in Figure 3.4.

Now that we have a uniquely defined unit cell in the reciprocal lattice, we only have to consider solutions which occur in this region, as all distinct Bloch waves occur within the first Brillouin zone. To simplify it even further, there is a related concept called the irreducible Brillouin zone, which is the first Brillouin zone reduced by the all of its symmetries. We first plot the isofrequency contours of all four of the eigenvalues across the whole of the first Brillouin zone in Figure 3.5. It is clear to see that there exists an eightfold symmetry and we can actually focus our attention on the region indicated in Figure 3.6, which is known as the irreducible Brillouin zone..

With these concepts, we can fully solve the dispersion relation over our infinite lattice space by just finding the solutions within the irreducible Brillouin zone. To simplify our analysis, we will just be solving the dispersion relation over the boundary of the irreducible Brillouin zone, i.e. we are taking slices of our dispersion relation over κ -space, as we can see it cuts through all the isofrequency contours we have.

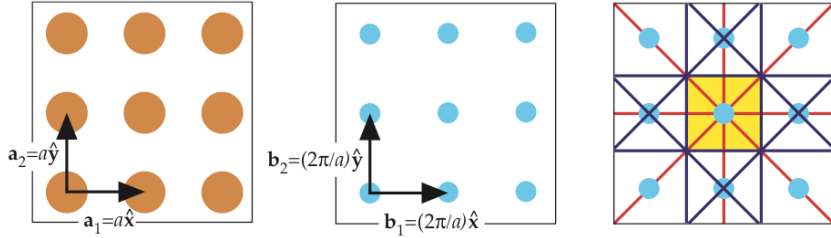


Figure 3.4: On the left is the lattice points in real space. In the middle is the corresponding reciprocal lattice. On the right is the construction of the first Brillouin zone: straight lines are drawn from the origin to the other lattice points (red), their perpendicular bisectors are the Bragg planes (blue), and the innermost region enclosed by the Bragg planes is the first Brillouin zone (yellow). Image and caption adapted from source.⁴⁷

Isofrequency contours of eigenvalues across Square Brillouin zone

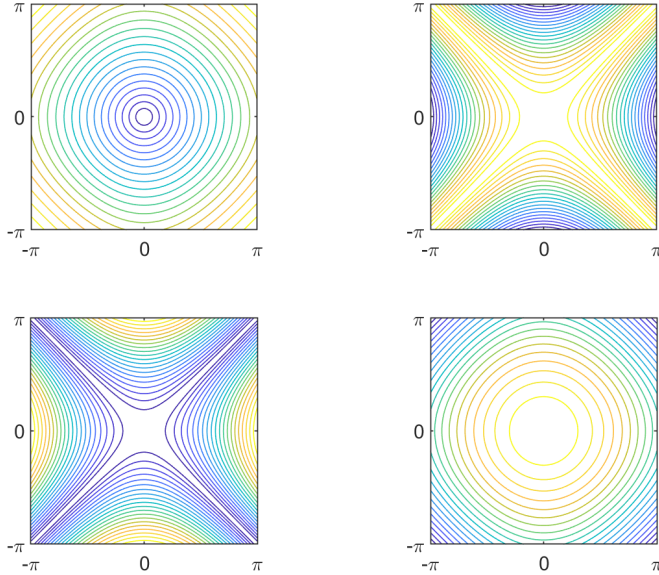


Figure 3.5: The isofrequency contours of the four eigenvalues across the first Brillouin zone of our square lattice with $M_i = k = \tilde{k} = 1$.

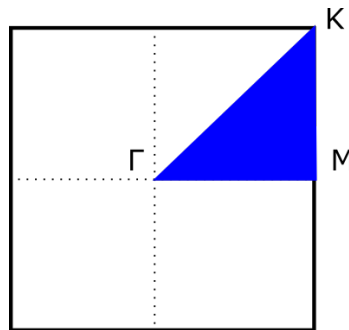


Figure 3.6: The irreducible Brillouin zone of the 2d square lattice in reciprocal space (blue).

Therefore for this case of an infinite 2d square lattice, we first solve the eigen-problem we have in (3.18) over the boundary of the irreducible Brillouin zone as shown in Figure 3.6. We do this in Matlab by varying the values of κ_x and κ_y which correspond to the locus of points on the boundary of the irreducible Brillouin zone, and then solve the eigen-problem for the eigenvalues and eigenvectors, which represent Ω and \vec{y} respectively. Then, we get the dispersion relation by

plotting out Ω_i against (κ_x, κ_y) or the position on the Brillouin zone.

Note: For Chapter 3 and 4, we will be focusing on analysing the eigenvalues to find the frequencies allowed to propagate in our system. Then we will make use of the eigenvectors y_i in Chapter 5 where we plot the values of y_i to visualise the propagation of waves through a finite lattice.

We first need to find the values of κ_x and κ_y at Γ , K and M as shown in Figure 3.6. Looking at reciprocal lattice vectors, we see that if our lattice vectors have length 1, then the reciprocal lattice vectors have length 2π . And we can see that $\Gamma = (0, 0)$, $K = (\pi, \pi)$ and $M = (0, \pi)$.

With this, and assuming that all masses $M_i = 1$ for now (we will explore how different perturbations in the lattice affect the dispersion relation in Chapter 4), we get the dispersion relation in Figure 3.7.

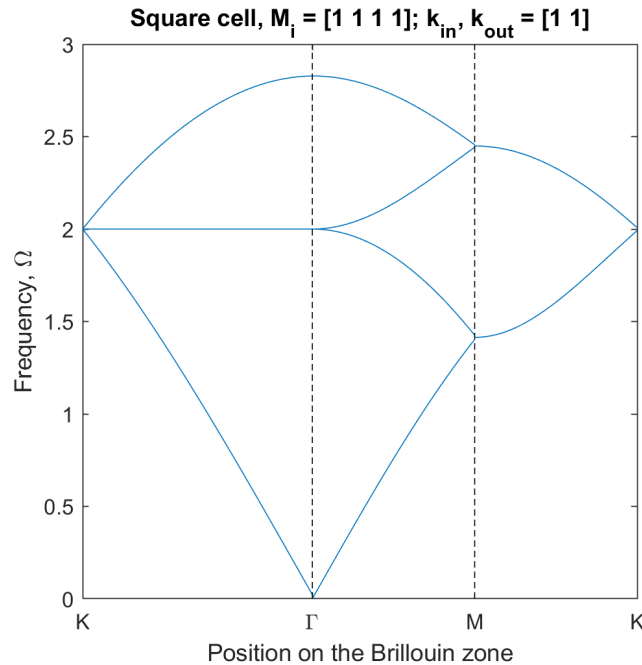


Figure 3.7: The dispersion relation of the 2d square lattice with $M_i = k = \tilde{k} = 1$.

It is important to note the *Dirac point* present at K where the two lines meeting are almost linear. The Dirac points where the dispersion curve touches will be important in Chapter 4 as those are the points at which we can form a bandgap and are what gives our edge states their special properties.

3.3 2d hexagonal lattice

We will now consider how waves propagate across a 2d lattice made of hexagonal elementary cells.

As described in Figure 3.8, consider an infinite 2d plane made of hexagonal unit cells of six masses M_i for $i \in [1, 6]$, which are arranged in an inner hexagon rotated $\frac{\pi}{6}$ relative to each cell.

Similarly to the 2d square lattice, we again consider only nearest neighbour interactions and focus on the elementary cell (n, m) and its adjacent cells. Using Hooke's law and Newton's 2nd law on each of the masses in cell (n, m) , we can get a second order differential equation which is coupled to the displacements of the other masses it is connected to. For example, considering $M_1^{n,m}$, we get

$$F_1 = M_1 \frac{d^2}{dt^2} y_1^{n,m} = k (y_2^{n,m} + y_6^{n,m} - 2y_1^{n,m}) + \tilde{k} (y_4^{n,m+1} - y_1^{n,m}) \quad (3.20)$$

Now again we can use the periodicity of the lattice and Bloch's theorem to relate the displacements of any mass to the displacement of the corresponding mass in a *base cell* using the lattice vectors shown in Figure 3.8:

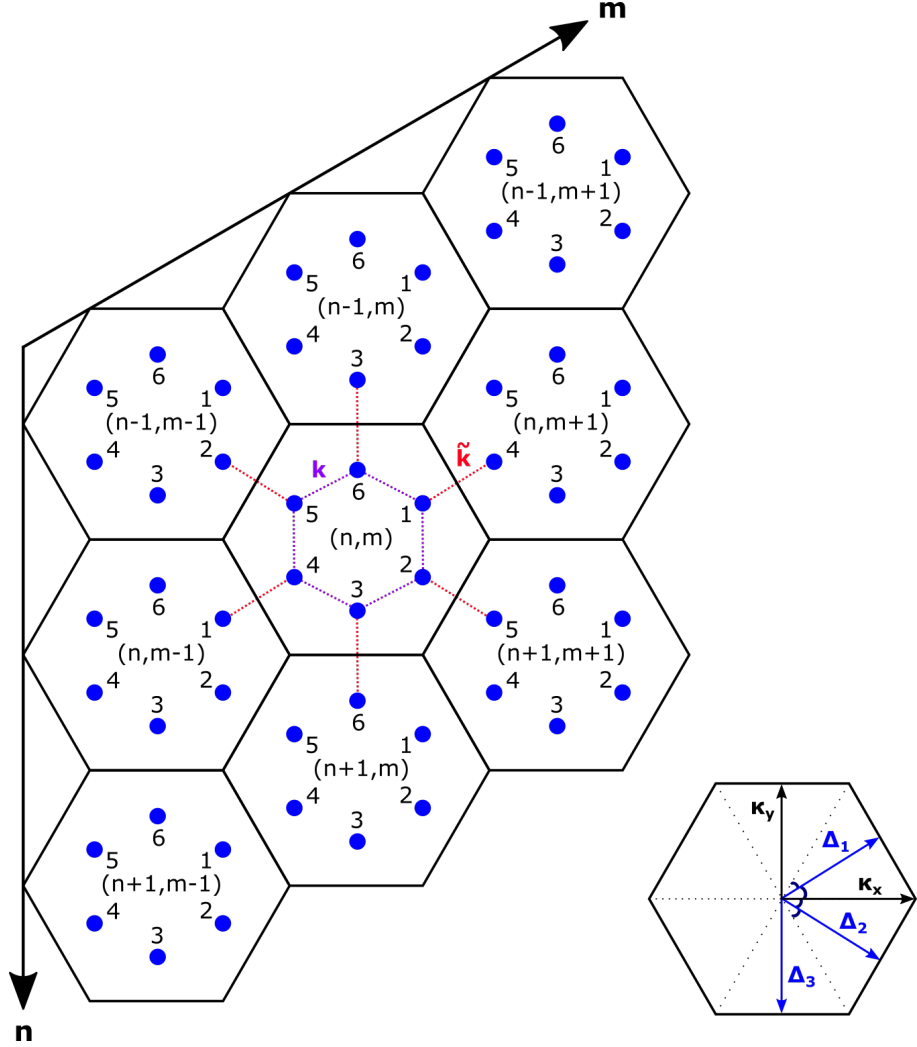


Figure 3.8: Schematic view of our 2d hexagonal model. Each hexagonal tile in the grid corresponds to one elementary cell with six masses. k and \tilde{k} represent the intra- and inter-cell spring constants respectively. The cell in the far bottom right shows the directions of the Bloch phases. Note that only the elastic interactions involving the masses in cell (n, m) are shown to avoid cluttering the figure, although they exist within and between each cell.

$$\Delta_1 = \sqrt{3}\kappa_x + \kappa_y \quad (3.21)$$

$$\Delta_2 = \sqrt{3}\kappa_x - \kappa_y \quad (3.22)$$

$$\Delta_3 = -2\kappa_y \quad (3.23)$$

With these, we can write out the relationship between the displacements for neighbouring cells, e.g. for cell (n, m) and its six nearest neighbours we have

$$y_4^{n,m+1} = e^{i\Delta_1} y_4^{n,m} \quad (3.24)$$

$$y_5^{n+1,m+1} = e^{i\Delta_2} y_5^{n,m} \quad (3.25)$$

$$y_6^{n+1,m} = e^{-i\Delta_3} y_6^{n,m} \quad (3.26)$$

$$y_1^{n,m-1} = e^{-i\Delta_1} y_1^{n,m} \quad (3.27)$$

$$y_2^{n-1,m-1} = e^{-i\Delta_2} y_2^{n,m} \quad (3.28)$$

$$y_3^{n-1,m} = e^{i\Delta_3} y_3^{n,m} \quad (3.29)$$

Using these, dropping the superscripts and again assuming we have a Bloch wave solution as described in (3.15), (3.20) can be rewritten as

$$M_1 \Omega_1^2 y_1 = (2k + \tilde{k}) y_1 - ky_2 - \tilde{k} e^{i\Delta_1} y_4 - ky_6 \quad (3.30)$$

Similarly to the 2d square model case, we can construct this equation for each y_i and then reformulate the six difference equations as an eigen-problem

$$[\mathbf{A}(\kappa_x, \kappa_y) - \boldsymbol{\Omega}\mathbf{M}] \vec{y} = \vec{0} \quad (3.31)$$

where $\boldsymbol{\Omega} = \text{diag}(\{\Omega_i^2\})$, $\mathbf{M} = \text{diag}(\{M_i\})$, $\vec{y} = [\{y_i\}]^T$ and now

$$\mathbf{A}(\kappa_x, \kappa_y) = \begin{bmatrix} 2k + \tilde{k} & -k & 0 & -\tilde{k} e^{i\Delta_1} & 0 & -k \\ -k & 2k + \tilde{k} & -k & 0 & -\tilde{k} e^{i\Delta_2} & 0 \\ 0 & -k & 2k + \tilde{k} & -k & 0 & -\tilde{k} e^{-i\Delta_3} \\ -\tilde{k} e^{-i\Delta_1} & 0 & -k & 2k + \tilde{k} & -k & 0 \\ 0 & -\tilde{k} e^{-i\Delta_2} & 0 & -k & 2k + \tilde{k} & -k \\ -k & 0 & -\tilde{k} e^{i\Delta_3} & 0 & -k & 2k + \tilde{k} \end{bmatrix} \quad (3.32)$$

Again, \mathbf{A} is Hermitian, guaranteeing that we get real eigenvalues, Ω . We will again use the theory of Brillouin zones as described in Chapter 2.7 to simplify the work we need to do in order to find the dispersion relation of this 2d hexagonal lattice.

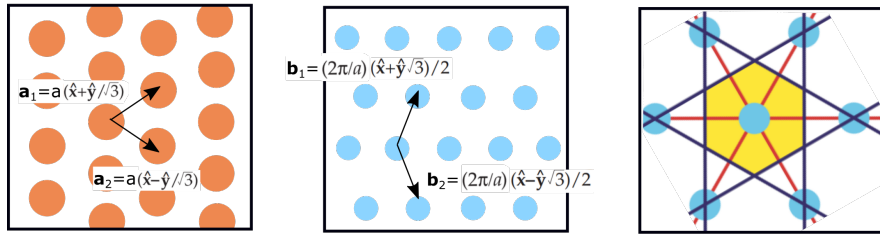


Figure 3.9: On the left is the lattice points in real space. In the middle is the corresponding reciprocal lattice. On the right is the construction of the first Brillouin zone: straight lines are drawn from the origin to the other lattice points (red), their perpendicular bisectors are the Bragg planes (blue), and the innermost region enclosed by the Bragg planes is the first Brillouin zone (yellow). Image and caption adapted from source.⁴⁷

So we have formed our first Brillouin zone in Figure 3.9. But again if we plot the isofrequency contours of the six eigenvalues across the entire zone as in Figure 3.10, we see that we have 12-fold symmetry!

So just as before, we can solve the dispersion relation over our infinite lattice by just solving it over the boundary of the irreducible Brillouin as shown in Figure 3.11, where we have $\Gamma = (0, 0)$, $K = (\frac{\pi}{\sqrt{3}}, \frac{\pi}{3})$ and $M = (\frac{\pi}{\sqrt{3}}, 0)$.

With this, and taking $M_i = k = \tilde{k} = 1$ for simplicity, we get the dispersion relation in Figure 3.12. Now we see that we have a few Dirac points, one at Γ and two at K , which we will break open later on.

Isofrequency contours of eigenvalues across Hex Brillouin zone

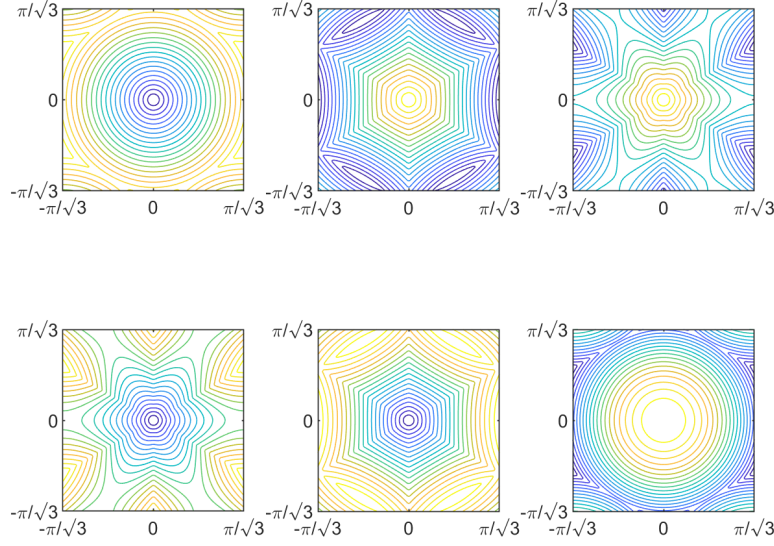


Figure 3.10: The isofrequency contours of the six eigenvalues across the first Brillouin zone of our hexagonal lattice with $M_i = k = \tilde{k} = 1$.

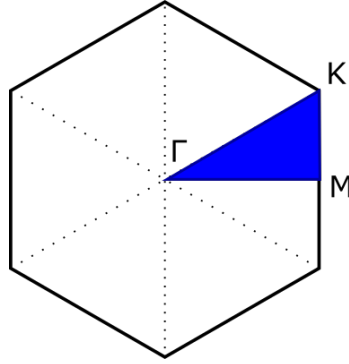


Figure 3.11: The irreducible Brillouin zone of the 2d hexagonal lattice in reciprocal space (blue).

3.4 2d kagome lattice

We will now investigate the kagome lattice in Figure 3.13, which is also known as the trihexagonal tiling as it consists of triangles surrounding hexagons, which can be seen in Figure 5.6.

Now again playing the same game as before, we can construct second order differential equations which couple the displacements of connected masses. For example, considering $M_1^{n,m}$, we get

$$F_1 = M_1 \frac{d^2}{dt^2} y_1^{n,m} = k(y_2^{n,m} + y_3^{n,m} - 2y_1^{n,m}) + \tilde{k}(y_2^{n-1,m} + y_3^{n,m+1} - 2y_1^{n,m}) \quad (3.33)$$

Due to the similarities in the shape of the elementary cell of the kagome lattice and the hexagonal lattice, the Bloch phases are the same and we can reuse (3.21), (3.22) and (3.23) as lattice vectors. In doing so, we find the following relationships:

$$y_1^{n+1,m} = e^{i\Delta_3} y_1^{n,m} \quad (3.34)$$

$$y_1^{n,m-1} = e^{-i\Delta_1} y_1^{n,m} \quad (3.35)$$

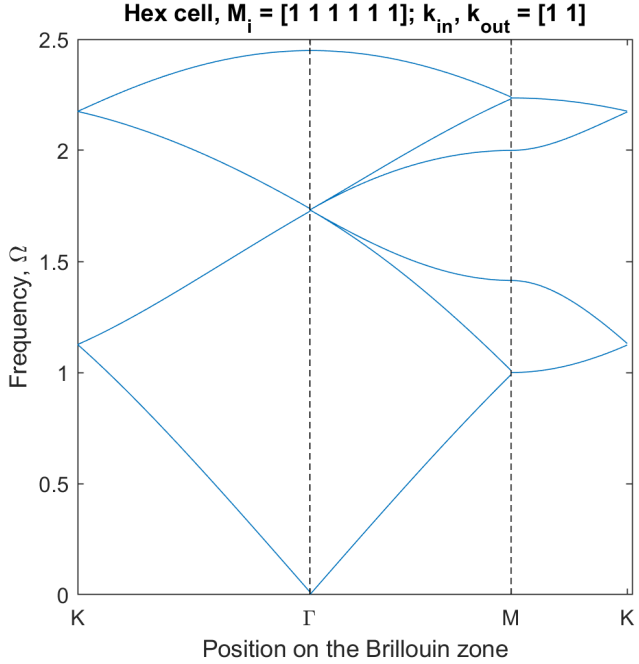


Figure 3.12: The dispersion relation of the 2d hexagonal lattice with $M_i = k = \tilde{k} = 1$.

$$y_2^{n-1,m} = e^{-i\Delta_3} y_2^{n,m} \quad (3.36)$$

$$y_2^{n-1,m-1} = e^{-i\Delta_2} y_2^{n,m} \quad (3.37)$$

$$y_3^{n,m+1} = e^{i\Delta_1} y_3^{n,m} \quad (3.38)$$

$$y_3^{n+1,m+1} = e^{i\Delta_2} y_3^{n,m} \quad (3.39)$$

With these, and assuming we have a Bloch wave solution as described in (3.15), we can rewrite (3.33) as

$$M_1 \Omega_1^2 y_1 = (2k + 2\tilde{k}) y_1 + (-k - \tilde{k}e^{-i\Delta_3}) y_2 + (-k - \tilde{k}e^{i\Delta_1}) y_3 \quad (3.40)$$

Again, by forming these equations for each of the three masses, and then combining them into one matrix equation, we get the following eigen-problem.

$$[\mathbf{A}(\kappa_x, \kappa_y) - \boldsymbol{\Omega}\mathbf{M}] \vec{y} = \vec{0} \quad (3.41)$$

where $\boldsymbol{\Omega} = \text{diag}(\{\Omega_i^2\})$, $\mathbf{M} = \text{diag}(\{M_i\})$, $\vec{y} = [\{y_i\}]^T$ and now

$$\mathbf{A}(\kappa_x, \kappa_y) = \begin{bmatrix} 2k + 2\tilde{k} & -k - \tilde{k}e^{-i\Delta_3} & -k - \tilde{k}e^{i\Delta_1} \\ -k - \tilde{k}e^{i\Delta_3} & 2k + 2\tilde{k} & -k - \tilde{k}e^{i\Delta_2} \\ -k - \tilde{k}e^{-i\Delta_1} & -k - \tilde{k}e^{-i\Delta_2} & 2k + 2\tilde{k} \end{bmatrix} \quad (3.42)$$

Again we have that \mathbf{A} is Hermitian and given the similarities in geometry between the kagome and hexagonal lattice, we see in Figure 3.14 that the irreducible Brillouin zones happen to be identical. Therefore, we can use the same zone as before, shown in Figure 3.15.

Note: The third eigenvalue found in Figure 3.14 is actually constant over the whole space, but is showing up as tiny random contours due to the small errors in the numerical solutions. As such,

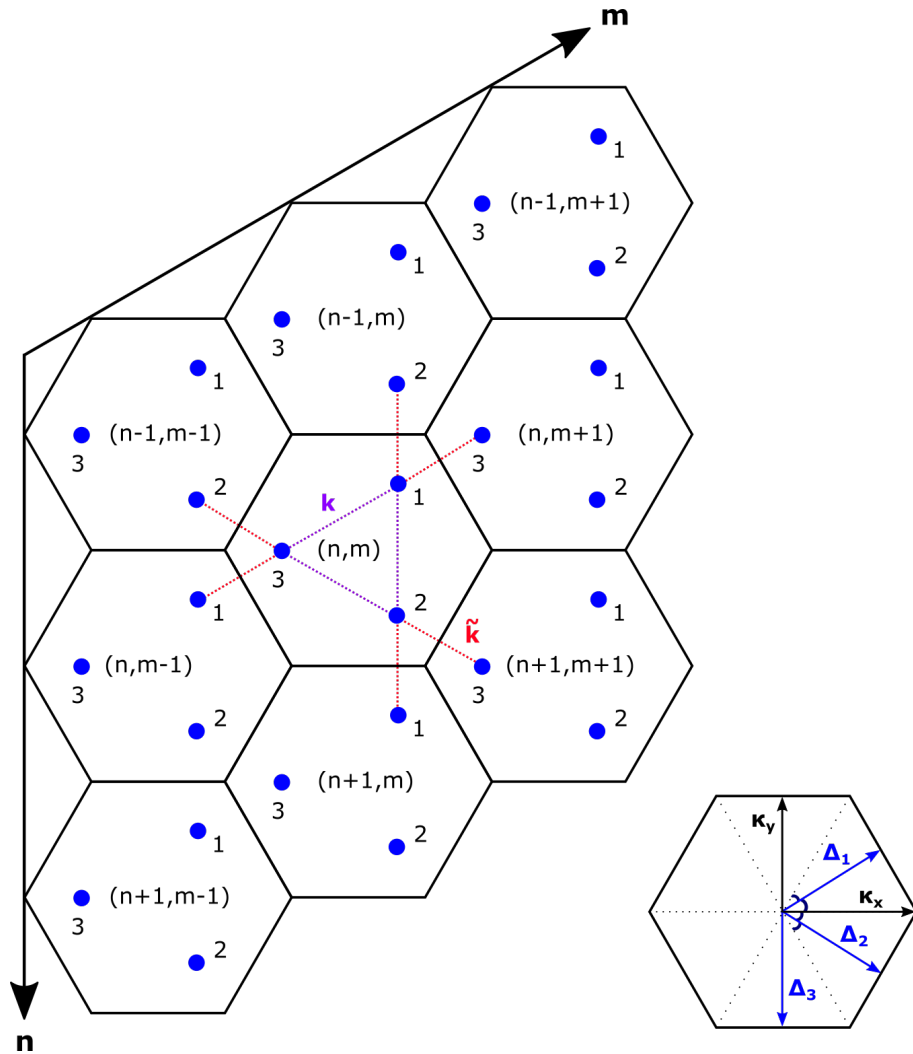


Figure 3.13: Schematic view of our 2d kagome model. Each hexagonal tile in the grid corresponds to one elementary cell with three masses. k and \tilde{k} represent the intra- and inter-cell spring constants respectively. The cell in the far bottom right shows the directions of the Bloch phases. Note that only the elastic interactions involving the masses in cell (n, m) are shown to avoid cluttering the figure, although they exist within and between each cell.

Isofrequency contours of eigenvalues across Kagome Brillouin zone

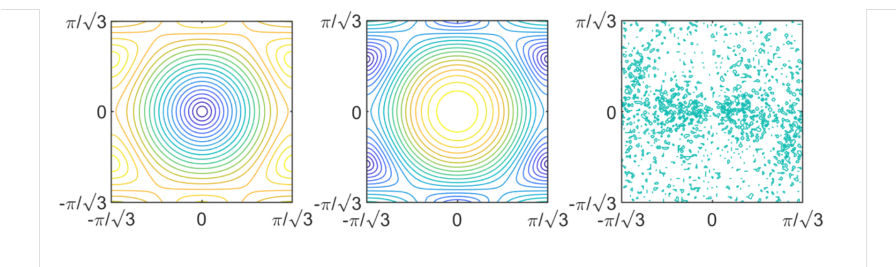


Figure 3.14: The isofrequency contours of the three eigenvalues across the first Brillouin zone of our kagome lattice with $M_i = k = \tilde{k} = 1$.

it also be restricted to the irreducible Brillouin zone. We will discuss further why it is constant later on.

By solving this eigen-problem along the boundaries of the irreducible Brillouin zone shown, we get the dispersion relation in Figure 3.16. Again, there is a Dirac point present at K .

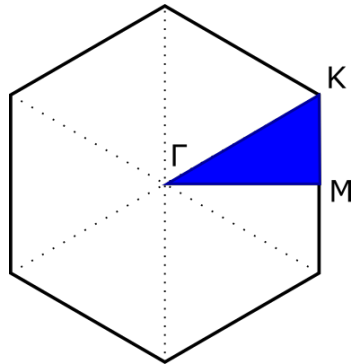


Figure 3.15: The irreducible Brillouin zone of the 2d kagome lattice in reciprocal space (blue).

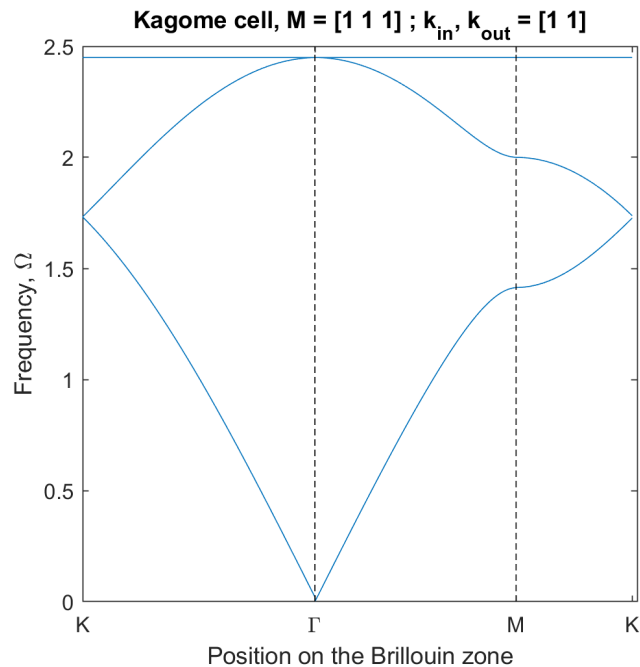


Figure 3.16: The dispersion relation of the 2d kagome lattice with $M_i = k = \tilde{k} = 1$.

What is really interesting about this dispersion relation is that there is one eigenvalue solution which is constant over the boundary of the irreducible Brillouin zone; but not only that, it is actually constant over the entire space as we have seen in the third eigenvalue shown in Figure 3.14! The value of this eigenvalue solution is actually constant at exactly $\sqrt{6}$. There are different classes of flat bands which have been studied,⁴⁹ and ours corresponds to the symmetry-protected chiral flat bands. We can see this is the case by breaking the cellular symmetry by perturbing the masses in each kagome cell, which can be seen in Figure 3.17. It is interesting to see that perturbing different masses breaks the flat band in different ways.

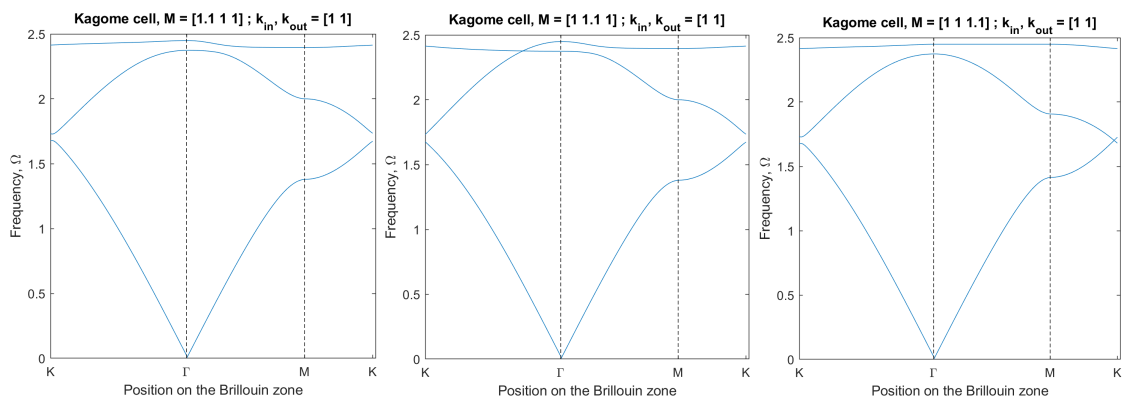


Figure 3.17: The dispersion relations of the 2d kagome lattice with one mass perturbed by 0.1 and all other parameters set to 1.

Chapter 4

Perturbed system

So far, we have seen how to compute the dispersion relation for some simple lattices. Now we want to see what sorts of effects we can create by introducing some perturbations. We will do this in terms of changing the masses as well as the spring constants between each mass in Chapter 4.2.2 and 4.4, and also alternating the masses in the hexagonal lattice in Chapter 4.2.1. Later on in Chapter 4.3 and 4.5, we will form a 2d strip or ribbon of these cells, with the top half possessing one set of properties and the bottom half possessing a different set of properties. We will see that this causes an edge state to occur at the boundary of the two halves.

Note: As the hexagonal and kagome lattices contain more symmetries due to the shape of their elementary cell, we will be focusing on perturbing these models, but the same can be done for the square lattice as well.

4.1 Band gap

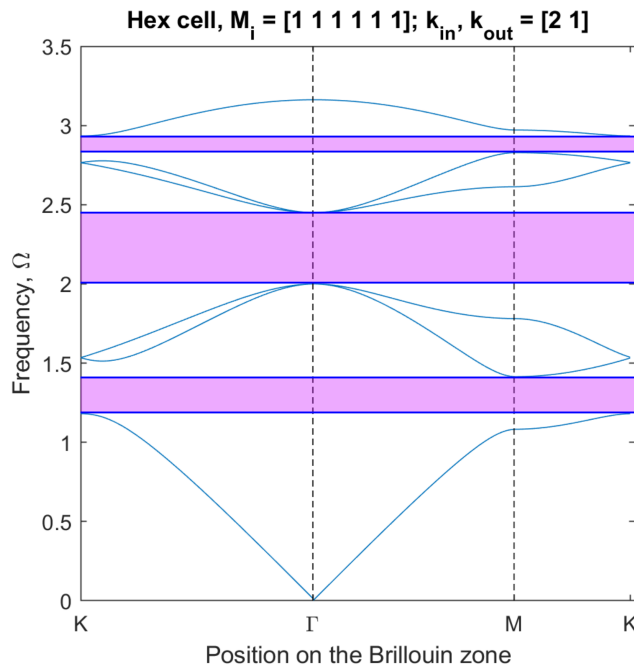


Figure 4.1: Example of bandgap (purple) formed in dispersion relation of hex lattice when $k = 2$ and $\tilde{k} = 1$.

A band gap, also called an energy gap, is an energy range where no wave states can exist. In terms of our lattices, this corresponds to a range of frequencies where waves are unable to propagate through the material; and in graphs of dispersion relations, it is seen as gaps in the frequency axis

where no line is present. An example is shown in Figure 4.1. Notice that the bandgaps are formed by the Dirac points breaking apart.

4.2 2d bulk hexagonal perturbation

Due to the many symmetries of the hexagonal lattice, there are many different ways for us to perturb its structure and break its symmetry. These all lead to slightly different effects on the dispersion relation.

4.2.1 Alternating masses

One way to perturb our bulk hexagonal lattice is by breaking one of its rotational symmetries. Currently our hexagonal lattice has six-fold rotational symmetry, i.e. rotating our cells by $\frac{2\pi}{6}$ do not change them. We can reduce this to a three-fold symmetry by alternating the masses such that $M_1 = M_3 = M_5 \neq M_2 = M_4 = M_6$.

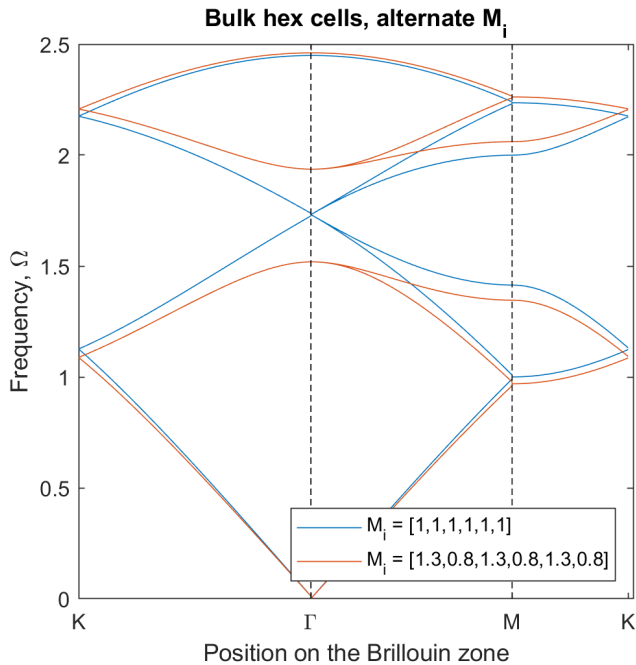


Figure 4.2: The effect of alternating the masses M_i on the dispersion relation of the bulk hexagonal system, with all other parameters set to 1.

In Figure 4.2, we see that alternating masses has opened up the Dirac point at Γ and formed a bandgap.

4.2.2 Varying mass and stiffnesses

Another way we can induce a bandgap in our system is by changing the ratio of the inner stiffness to the outer stiffness. This not only breaks one of the local symmetries (local in the sense of the individual cell) but also breaks one of the *global* symmetries that we get. This perturbation is an analogue to what is presented in this paper on photonic crystals.⁴³ This allows us to evaluate the validity and applicability of our system to modelling more complex systems and is what we focus on in Chapter 7.1.

If you look at our hexagonal lattice and focus on the springs connecting our masses, you can see that we have two different hexagons being formed, one within each cell and also another between three adjacent cells meeting at a vertex. When we have $k = \tilde{k}$, the inner and outer springs "tug" on the masses the same amount, and so the two different hexagons we were talking about before are of exactly the same proportions. However, when we modify our system such that the inner stiffness is greater, say, than the outer stiffness, the inner hexagons within each cell will be more

"tightly pulled in" on itself and in turn causing the outer hexagons to become bigger. This is shown in Figure 4.3.

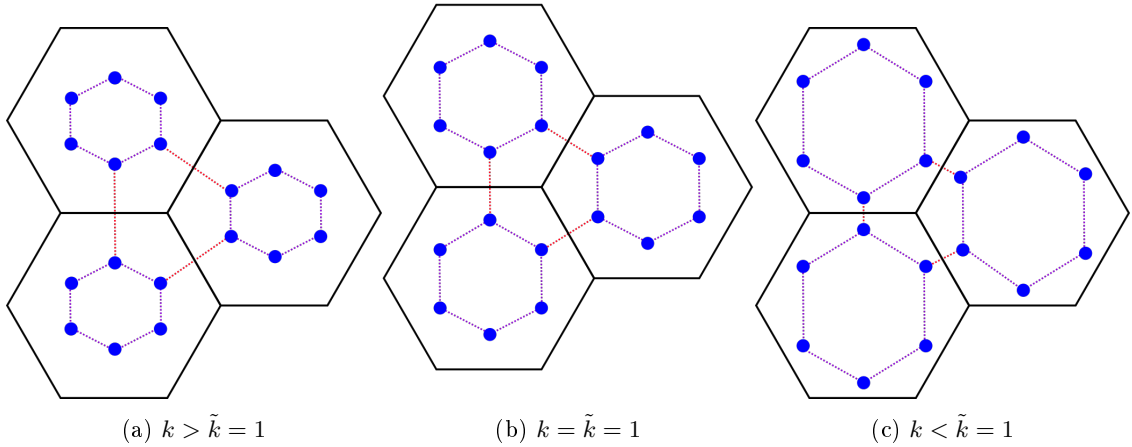


Figure 4.3: The effect of varying k on the sizes of the inner and outer hexagons in the hexagonal lattice.

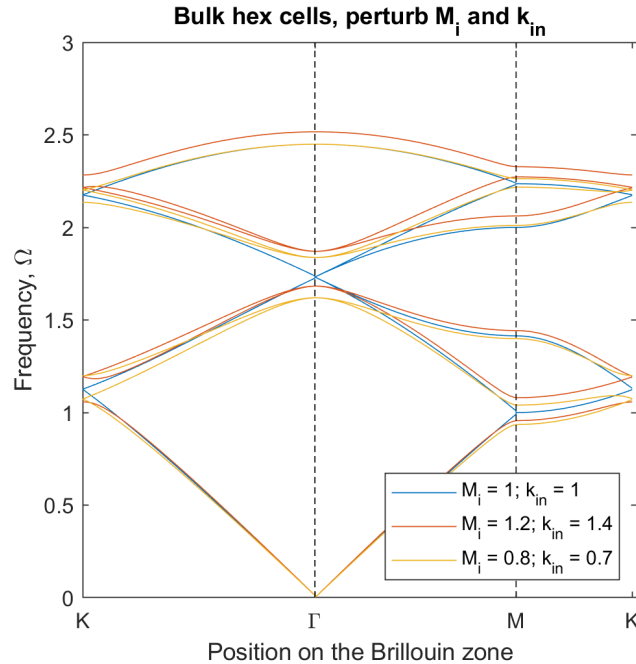


Figure 4.4: The effect of perturbing the masses M_i and k on the dispersion relation of the bulk hexagonal system, with all other parameters set to 1.

Very interestingly, we can see in Figure 4.4 that increasing both the mass and inner stiffness as well as decreasing both the mass and inner stiffness leads to the formation of three bandgaps. This means that this time we break all three Dirac points! We take a closer look at how changing M_i and changing k individually affect the dispersion relation in the kagome lattice in Chapter 4.4.

4.3 2d hexagonal strip

Now we assemble $2N$ hexagonal cells together into a strip and form a semi-infinite hexagonal lattice by joining these strips from side-to-side as shown in Figure 4.5. We will subscript the values corresponding to the top half and bottom half with t and b respectively, e.g. k_t to refer to the

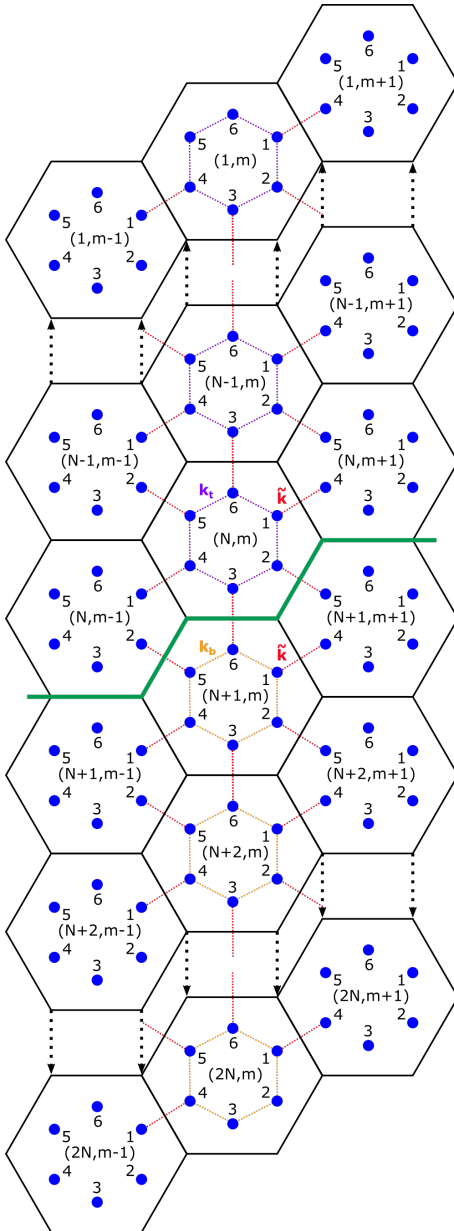


Figure 4.5: Schematic view of the 2d hexagonal semi-infinite lattice made from an infinite number of strips connected side-by-side. Each strip is composed of $2N$ cells, with the top half of cells above the boundary (green) possessing a set of properties and the bottom half possessing a separate set of properties. Note the boundary conditions at the top and bottom, i.e. the cells at the top and bottom edges have no connections outside the lattice.

inner spring constants for the top half and $M_{1,b}$ to refer to the mass of mass 1 in the bottom half. We set the outer spring constant, $\tilde{k}_t = \tilde{k}_b = \tilde{k}$ to be the same throughout the strip, to ensure that it agrees on both sides of the boundary or interface.

Using the same reasonings in Chapter 3.3 to form equations between adjacent cells, we can also form an eigen-problem as before (where the size of our matrix is now $(2N \times 6) \times (2N \times 6)$ instead of 6×6). The only difference and extra care we have to take is to insert the right coupling terms between masses in different cells, e.g. M_3 is not connected to M_6 displaced by some phase shift anymore, but is connected to M_6 in the cell below.

Also, we explicitly choose the boundary condition where the top and bottom cells have no connections outside the lattice. This is similar to having our top and bottom edges connected to a *rigid wall* as our waves are unable to leave the lattice from those two edges. This is important to note as the rigid boundary gives rise to a different dispersion curve at the top and bottom

boundaries which can lead to propagation of waves that we do not want, such as in Figure 6.1d.

Note: Another sensible periodic boundary condition which we could have imposed at the top and bottom edges is by coupling the top and bottom cells together across the edge. Specifically, we could impose

$$\mathbf{A}_{6,6(2N-1)+3} = \mathbf{A}_{6(2N-1)+3,6} = -\tilde{k} \quad (4.1)$$

$$\mathbf{A}_{5,6(2N-1)+2} = -\tilde{k}e^{-i\Delta_1} \quad (4.2)$$

$$\mathbf{A}_{6(2N-1)+2,5} = -\tilde{k}e^{i\Delta_1} \quad (4.3)$$

This essentially gives us an infinite lattice going from top to bottom, with top and bottom materials alternating. Therefore essentially, the significant difference which we will see between the two boundary conditions is that one models the top and bottom edge as edges between our materials and a rigid wall, and the other models the top and bottom edge as edges between our two materials. However, we will see later on that this will not matter too much for our scattering simulations as we will be exciting waves of frequencies in our bandgaps. So if we take N to be large enough, the exponential decay of the wavefunctions across the strip is great enough to ensure our wave does not propagate to the top and bottom edges anyways.

With that out of the way, we can finally form the eigen-problem

$$[\mathbf{A}(\kappa_x, \kappa_y) - \Omega \mathbf{M}] \vec{y} = \vec{0} \quad (4.4)$$

where \mathbf{A} is a $(2N \times 6) \times (2N \times 6)$ matrix with \mathbf{A} as defined in (3.31) repeated along the diagonal and with the additional coupling terms added, $\Omega = \text{diag}(\{\Omega_i^2\})$, $\mathbf{M}_t = \text{diag}(\{M_{i,t}\})$, $\mathbf{M}_b = \text{diag}(\{M_{i,b}\})$,

$$\mathbf{M} = \begin{bmatrix} \mathbf{M}_t & & & & & \\ & \ddots & & & & 0 \\ & & \mathbf{M}_t & & & \\ & & & \mathbf{M}_b & & \\ & 0 & & & \ddots & \\ & & & & & \mathbf{M}_b \end{bmatrix}, \quad (4.5)$$

$$\vec{y} = \begin{bmatrix} y_1^{(1)} \\ \vdots \\ y_6^{(1)} \\ \vdots \\ y_1^{(2N)} \\ \vdots \\ y_6^{(2N)} \end{bmatrix}, \quad (4.6)$$

Now with this eigen-problem, all we have left to do is figure out what region of the reciprocal space we should solve over for our ribbon system. Since we are interested only in waves which are propagated along the interface of our ribbon system, we need only consider Bloch conditions in the direction of the arrow indicated in Figure 4.6.

Therefore, limiting ourselves to a single reciprocal cell, we go from $K' = (-\frac{\sqrt{3}\pi}{4}, -\frac{pi}{4})$ to $\Gamma = (0, 0)$ to $K = (\frac{\sqrt{3}\pi}{4}, \frac{pi}{4})$.

Solving this with $M_{i,t} = M_{i,b} = k_t = k_b = \tilde{k} = 1$ over the irreducible Brillouin zone gives us the dispersion relation in Figure 4.7, which corresponds to what we see in Figure 3.12 (if you take the graph from K to Γ and then reflect it about the vertical at Γ).

As we have just done in Chapter 4.3, we will see what happens to the dispersion relation when we set the two layers of the lattice to have different properties as those before which opened up a band gap.

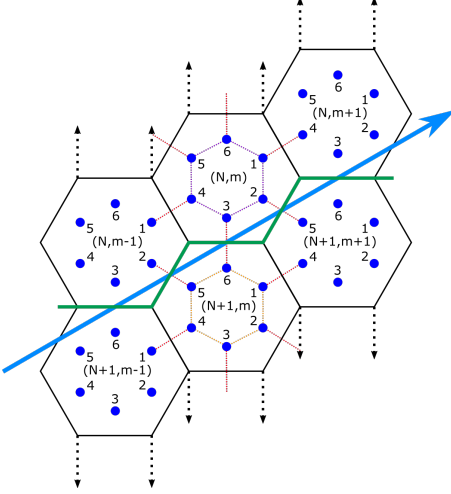


Figure 4.6: Direction of Bloch conditions (blue arrow) we need to consider for our hexagonal ribbon system.

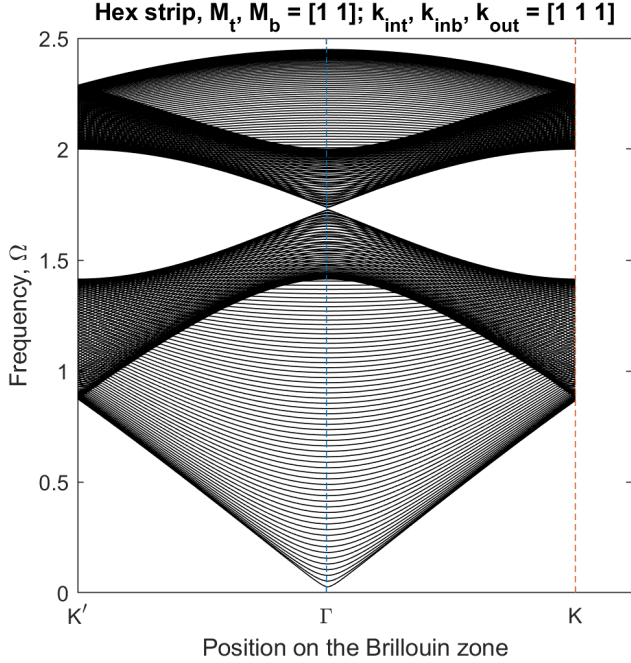


Figure 4.7: Dispersion relation of the semi-infinite hexagonal lattice with $2N = 40$ (40 cells in total) with $M_{i,t} = M_{i,b} = k_t = k_b = \tilde{k} = 1$.

4.3.1 Alternating masses

Using our results of the formation of a bandgap in, let us first see what happens when we create a hexagonal strip where the top and bottom have the same property of alternating masses.

Again, we see in Figure 4.8 that basically the dispersion relation we get corresponds to that of Figure 4.2 (if you look at the graph from K to Γ and reflect about Γ), where there is a bandgap present. This is all fine and good but we can do something even better.

In this system, the two layers of materials are the same which means that essentially it behaves just like the bulk hexagon case. It is as if we just took a finite chunk of the infinite bulk lattice. So with that in mind, let us change the bottom layer into a different configuration. The easiest way of perturbing it so that we still get the exact same dispersion relation in the bulk case is to rotate the cell by $\frac{2\pi}{6}$. This is because locally (at the cellular level), nothing has changed and if we form a bulk system from the rotated cell we still get the same bulk system but rotated, but this does not affect the frequencies of waves allowed to propagate. So even if we stack the two different types

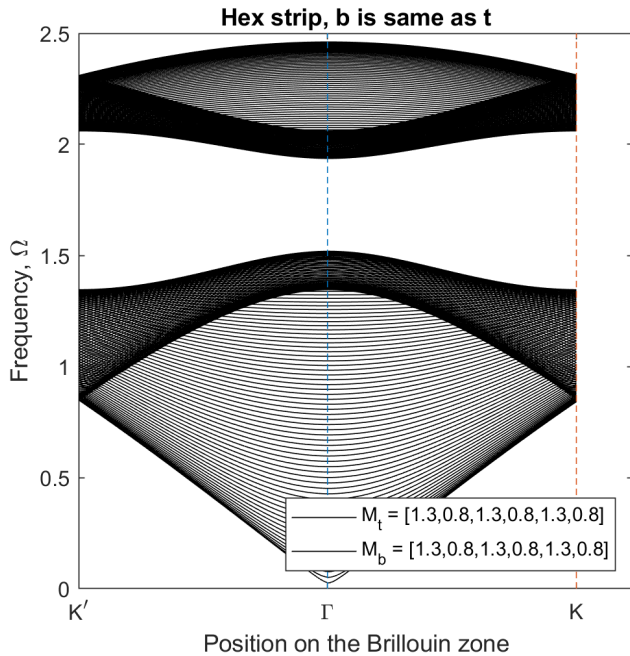


Figure 4.8: Dispersion relation of the semi-infinite hexagonal lattice with alternating masses (with the top and bottom layer the same configuration), with all other parameters set to 1.

of cells on each other, we would expect the same bandgap to be present, since locally each cell exhibits that property. However if we now consider the global symmetry when stacking the two different materials on top of each other, we can see that we have broken some sort of translational symmetry and so would expect something different in the dispersion relation.

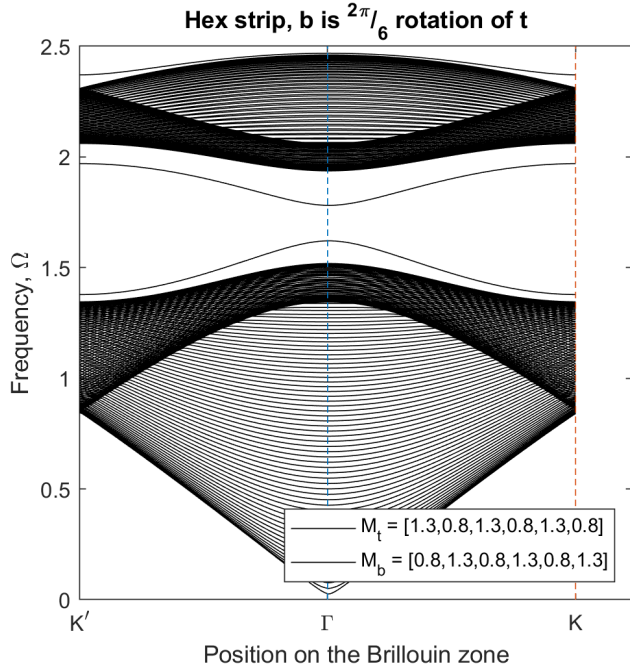


Figure 4.9: Dispersion relation of the semi-infinite hexagonal lattice with alternating masses (with bottom layer as a $\frac{2\pi}{6}$ rotation of the top layer), with all other parameters set to 1.

As expected, we see that in Figure 4.9 we get pretty much the same dispersion relation as in Figure 4.8 but with two curious lines in the bandgap! This is really interesting and useful for us because this means that all the frequencies along the two lines in the bandgap are only

able to propagate along the centre line of the semi-infinite lattice we constructed, i.e. along the boundary and not anywhere else in the lattice. The waves corresponding to the waves of these special frequencies are known as the edge modes or edge states of our system, as they travel *along the edge* or boundary and exponentially decay outwards from that edge. With this knowledge, we are then able to start trying to force energy to propagate in the directions we desire in Chapter 5.

4.3.2 Varying mass and stiffnesses

We can do the same thing in this case, but instead of making the bottom layer a rotation of the top layer, we make the top have a greater M_i and k and the bottom have a lower M_i and k . As we have seen in Figure 4.4, we have one increased and one decreased system which have similar bandgaps. As such, we will be using those two configurations to form our strip.

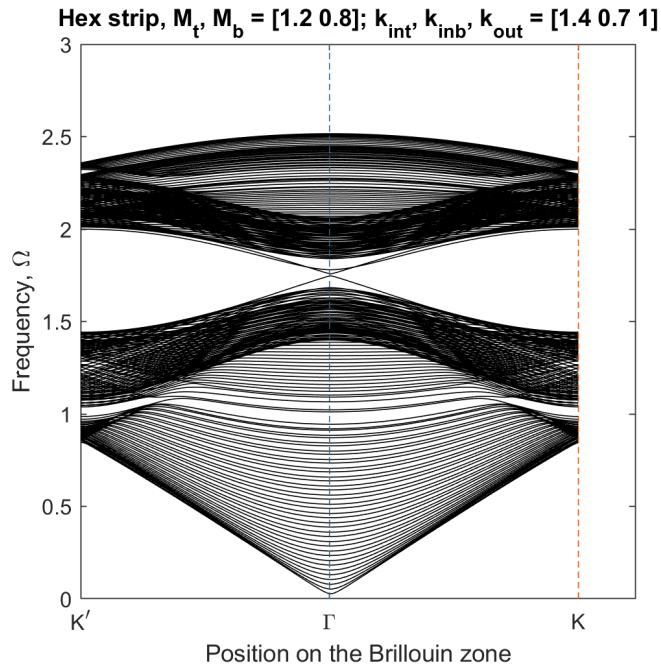


Figure 4.10: Dispersion relation of the semi-infinite hexagonal lattice where the top material has a higher M_i and k than the bottom material, with all other parameters set to 1.

As before we again get a well-defined bandgap, as well as two dispersion lines which are present in the bandgap and therefore correspond to edge states.

4.4 2d bulk kagome perturbation

Similarly to the hexagonal case, we can perturb the different parameters in our bulk kagome system to see what effects they have on the dispersion relation.

We can see the effects that perturbing the masses M_i and inner stiffness k have on the bulk kagome system. In the case of varying M_i in Figure 4.11, increasing M_i decreases or constrains the dispersion relation, while decreasing M_i increases or widens the dispersion relation.

However, in the case of varying k in Figure 4.12, we see the inverse effect; increasing k increases or widens the dispersion relation, while decreasing k decreases or constrains the dispersion relation. Another interesting thing to notice about changing k is that it opens up the Dirac point at K and causes the formation of a bandgap!

With these two inverse relationships, we are naturally propelled to ask what happens if we combine both of these effects together. For example, by increasing M_i and increasing k , would the two effects *cancel out* to give us the same dispersion relation as the unperturbed system? That is precisely what happens and can be seen in Figure 4.13 as well as Figure 4.4.

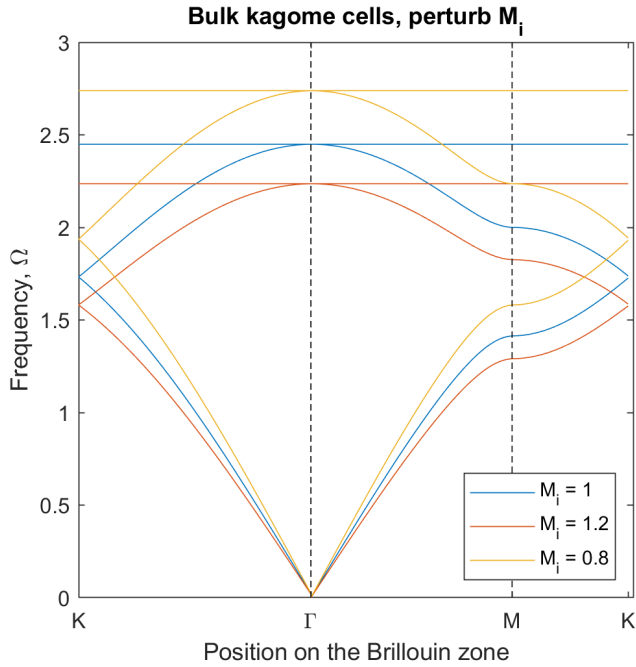


Figure 4.11: The effect of perturbing the masses M_i on the dispersion relation of the bulk kagome system, with all other parameters set to 1.

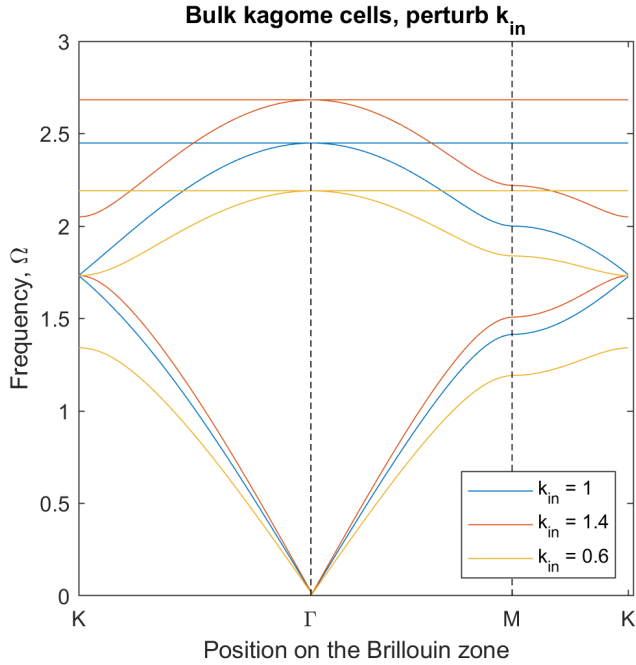


Figure 4.12: The effect of perturbing the inner stiffness k on the dispersion relation of the bulk kagome system, with all other parameters set to 1.

4.5 2d kagome strip

As we have just done in the hexagonal case, we assemble $2N$ kagome cells together into a strip and form a semi-infinite lattice with these strips connected left-to-right as shown in Figure 4.14.

Using the same conventions as the hexagonal strip case and similarly imposing rigid boundary conditions at the top and bottom edge, we can form the eigen-problem

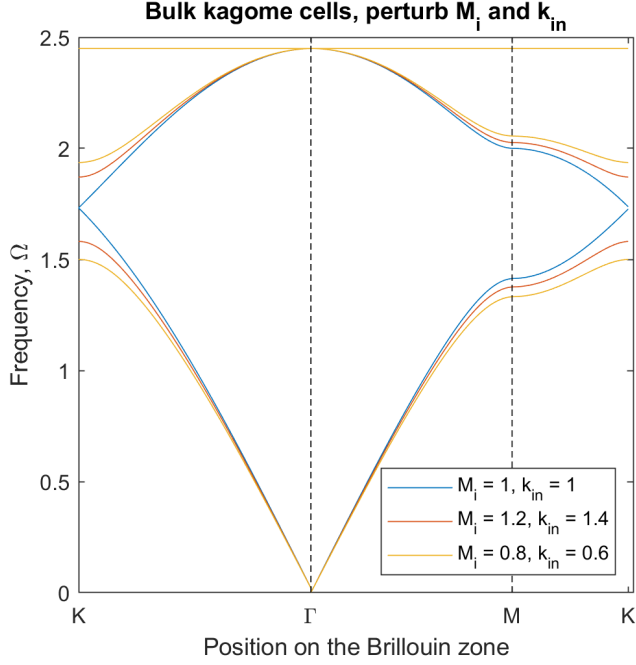


Figure 4.13: The effect of perturbing both the masses M_i and the inner stiffness k on the dispersion relation of the bulk kagome system, with all other parameters set to 1.

$$[\mathbf{A}(\kappa_x, \kappa_y) - \boldsymbol{\Omega}\mathbf{M}] \vec{y} = \vec{0} \quad (4.7)$$

where \mathbf{A} is a $(2N \times 6) \times (2N \times 6)$ matrix with \mathbf{A} as defined in (3.41) repeated along the diagonal and with the additional coupling terms added, $\boldsymbol{\Omega} = \text{diag}(\{\Omega_i^2\})$, $\mathbf{M}_t = \text{diag}(\{M_{i,t}\})$, $\mathbf{M}_b = \text{diag}(\{M_{i,b}\})$,

$$\mathbf{M} = \begin{bmatrix} \mathbf{M}_t & & & & & \\ & \ddots & & & & 0 \\ & & \mathbf{M}_t & & & \\ & & & \mathbf{M}_b & & \\ 0 & & & & \ddots & \\ & & & & & \mathbf{M}_b \end{bmatrix}, \quad (4.8)$$

$$\vec{y} = \begin{bmatrix} y_1^{(1)} \\ y_2^{(1)} \\ y_3^{(1)} \\ \vdots \\ y_1^{(2N)} \\ y_2^{(2N)} \\ y_3^{(2N)} \end{bmatrix}, \quad (4.9)$$

Solving this with $M_{i,t} = M_{i,b} = k_t = k_b = \tilde{k} = 1$ over the same κ -space as the hexagonal system (since they are built from the same elementary hexagonal cell), gives us the dispersion relation in Figure 4.15.

Now let us try to get the dispersion relation for the semi-infinite kagome lattice where the top material is made of the kagome cells with increased M_i and k and the bottom material is made of kagome cells decreased M_i and k , as we used in Figure 4.13.

Again, as in the hexagonal case, we have a bandgap with two well-defined dispersion curves corresponding to edge states which live on the boundary.

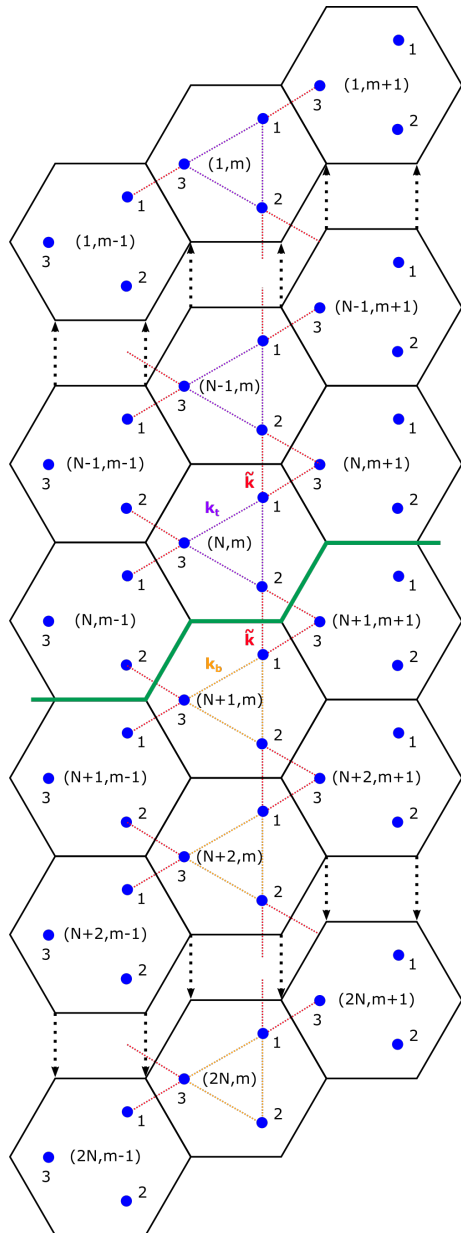


Figure 4.14: Schematic view of the 2d kagome semi-infinite lattice made from an infinite number of strips connected side-by-side. Each strip is composed of $2N$ cells, with the top half of cells above the boundary (green) possessing a set of properties and the bottom half possessing a separate set of properties.

Also, one thing interesting to note is that even with our perturbations, in both the bulk and strip case we still have a flat band, as we have not broken the symmetry of the cell as mentioned before!⁴⁹

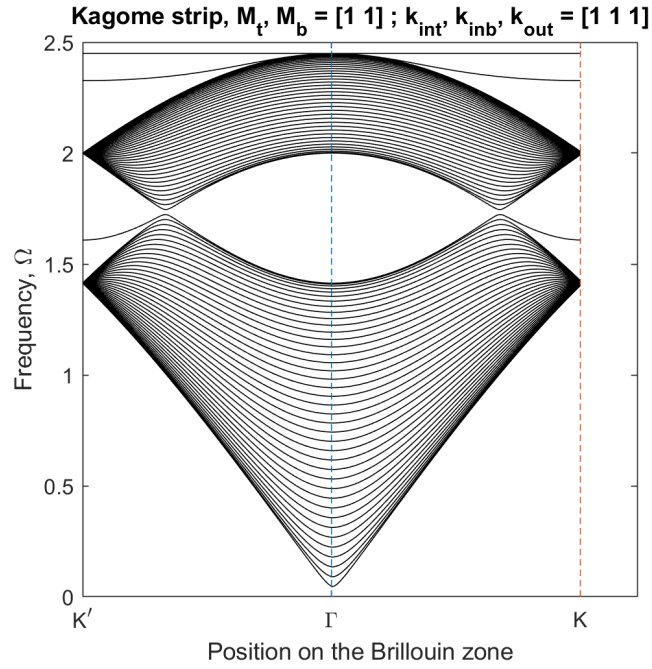


Figure 4.15: Dispersion relation of the semi-infinite kagome lattice with $2N = 40$ (40 cells in total) with $M_{i,t} = M_{i,b} = k_t = k_b = \bar{k} = 1$.

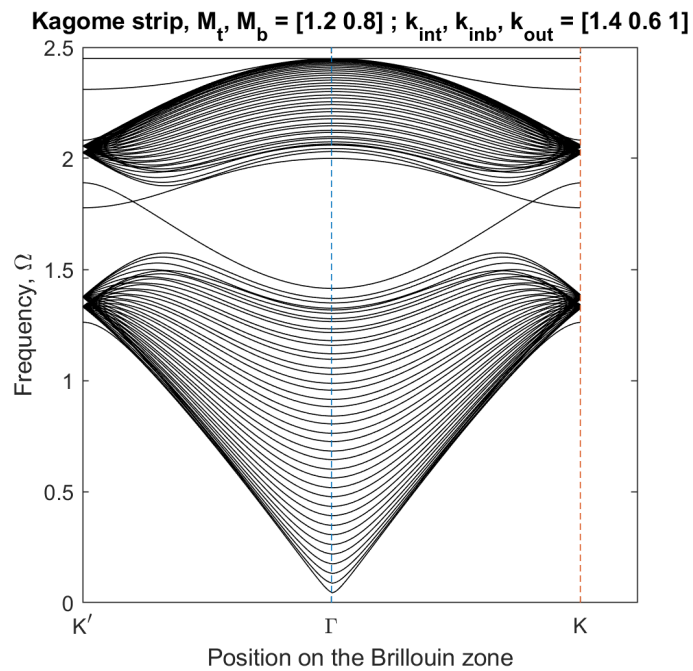


Figure 4.16: Dispersion relation of the semi-infinite kagome lattice where the top material has a higher M_i and k than the bottom material, with all other parameters set to 1.

Chapter 5

Scattering simulation

Finally after all our hard work of investigating the dispersion curves of different lattices as well as finding out how to perturb them such that we form a bandgap, we will actually simulate how a wave of a certain frequency propagates and scatters through a finite portion of one of our lattices.

Similarly to how we joined cells together to form a strip, we will do the same and join strips to form a finite lattice. We may then reframe our eigen-problem systems in reciprocal space into linear systems in physical space. From there, we can solve the linear systems to see how the energy or wave moves throughout the entire space. All we need to do is pick a frequency for the wave we want to simulate as well as where we want the source of excitation to be.

From the dispersion relations, we know which frequency waves are able to propagate across the lattice and which frequencies are not transmitted through the lattice. As we have discussed before in Chapter 4.3, we know that there are certain frequencies which are only able to propagate along the interface of the strips and not anywhere else in the lattice. These are the frequencies which we will be simulating.

5.1 Our linear system in physical space

Before we can run our scattering simulations, which essentially is solving for the displacements of masses in our finite lattice, we need to form the system to solve. This actually turns out to be really similar to the eigen-problems we had earlier (albeit with a much larger matrix involved!). It is also useful to note that the following derivation works just as well for systems of any shape as long as we have formed the eigen-problem as before, as we will reuse the variables in the eigen-problem here.

We will show it for the hexagonal lattice. Looking at (4.4), we first need to extend the system to include our whole finite lattice which is formed by joining strips side-by-side. So now \mathbf{A} is a $(2N \times M \times 6) \times (2N \times M \times 6)$ matrix with \mathbf{A} from (4.4) repeated M times along the diagonal, with the complex exponential terms removed and additional coupling terms between masses in adjacent strips added in. We also extend \mathbf{M} by repeating \mathbf{M} M times along the diagonal.

The key idea now is just to notice that when we can pick and choose the frequency, Ω , the LHS $[\mathbf{A}(\kappa_x, \kappa_y) - \Omega \mathbf{M}] = \mathbf{B}$ just falls out as a known-valued matrix. Then for the RHS, instead of $\vec{0}$, we will have a vector \vec{F} containing our forcing terms at the masses which will act as our source of excitation, e.g. if we are inducing a positive wave at the mass $M_i^{n,m}$, then we will have \vec{F} is a vector of 0 except at the position which corresponds to mass $M_i^{n,m}$ we will have a 1. Then we see

$$\mathbf{B}\vec{y} = \vec{F} \tag{5.1}$$

which is just a linear system we can solve for \vec{y} !

With this linear system set up, let us take a look at the physical spaces in which we will run these simulations.

5.2 2d hexagonal finite lattice

Figure 5.1 shows a schematic view of the finite hexagonal lattice on which we are simulating our scattering. Specifically, we will be running our following simulations on the arrangement of cells in

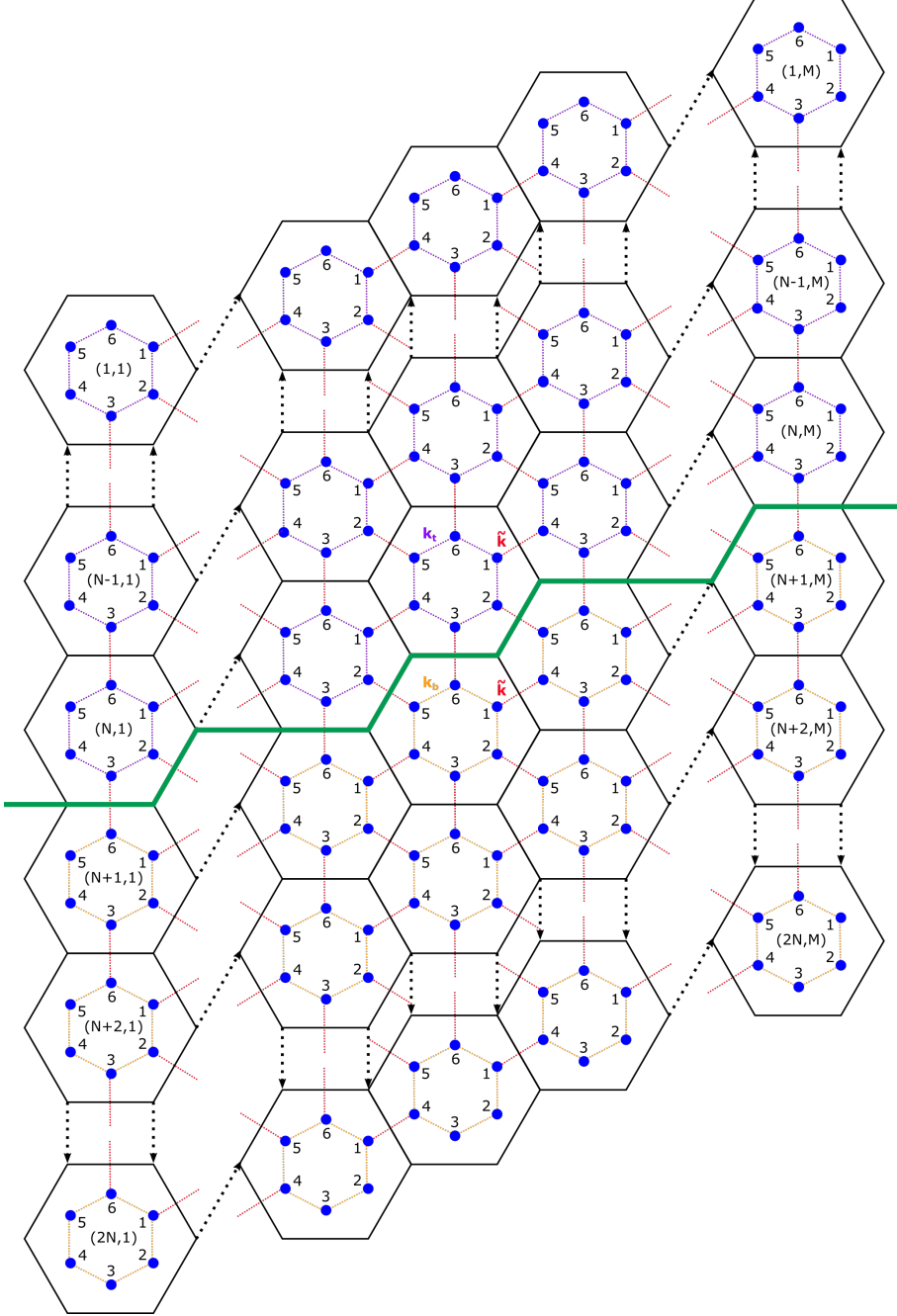


Figure 5.1: Schematic view of the finite hexagonal lattice formed from the joining of strips side-by-side, where the strips themselves are formed from two different halves as in Chapter 4. Note the conditions imposed at the boundaries (masses at boundaries have no connections outside the lattice).

Figure 5.2. We will be exciting our lattice at the leftmost edge of the boundary. More specifically, we will have a positive excitation just above the boundary (at M_4), and a negative excitation just below the boundary (at M_5), i.e. \vec{F} is 0 everywhere except $\vec{F}_{6(\frac{N}{2}-1)+4} = 1$ and $\vec{F}_{6(\frac{N}{2})+5} = -1$.

5.2.1 Alternating masses

In this section we will run scattering simulations on the physical lattice as described in Chapter 4.3.1 with the alternating masses.

Now, we can run our simulations for another frequency we want, but we know from our dispersion relations that most frequencies (those outside the special dispersion curves corresponding to

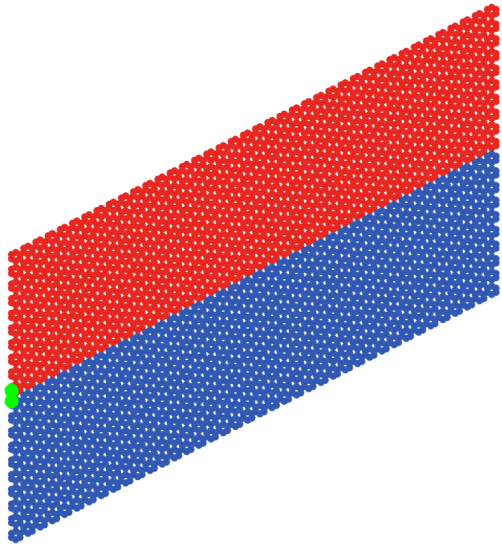


Figure 5.2: Arrangement of hexagonal cells ($2N = 20, M = 40$), with red and blue being different materials, and source of excitation at the green masses.

the edge states) will just propagate throughout the lattice and so we would not get any discernible patterns of movement. An example can be found in Figure 5.3.

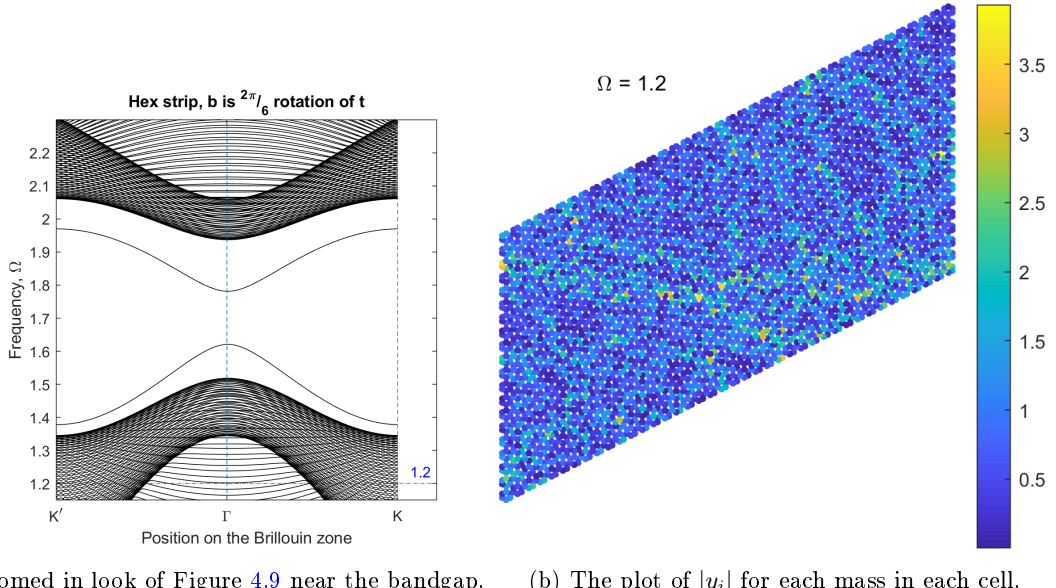
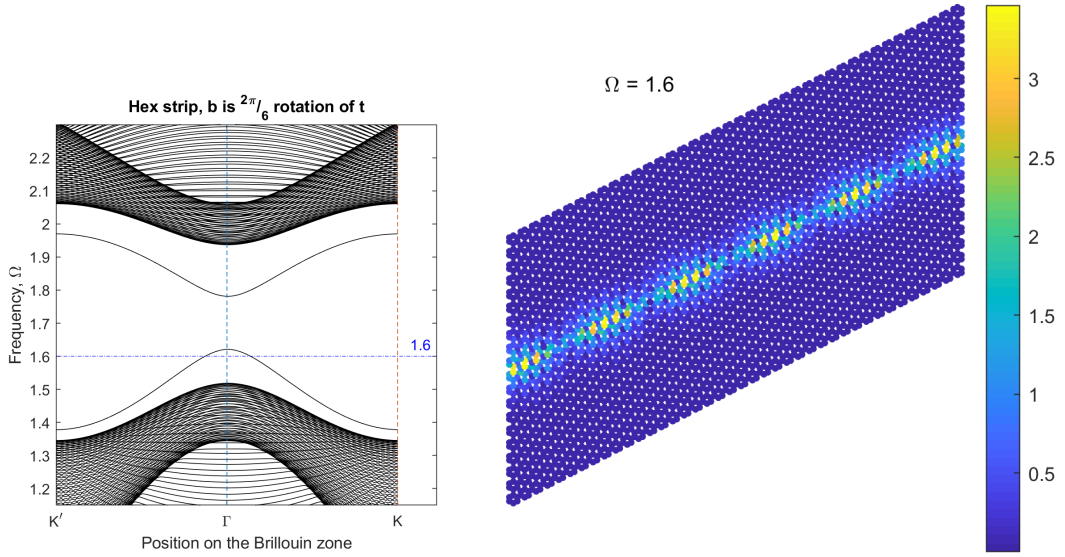


Figure 5.3: Simulation of scattering on the hexagonal finite lattice in Figure 5.2 with the alternating masses as defined in Figure 4.9 with $\Omega = 1.2$.

As we are interested in being able to direct waves to our liking, it is much more exciting to fire a frequency which is only able to travel along the boundary. So let us use the same system as in Figure 5.3 again, but using $\Omega = 1.6$ instead as we can see in Figure 5.4a that the dispersion curve for that edge mode lives in the bandgap.

Wonderful! Finally after all our hard work we can see in Figure 5.4 that the wave or energy forced into the system is only propagating along the straight line. This effectively means that we can control the direction of propagation of waves through our lattice and not have it diffuse or leak out into the other parts of the lattice. Of course our next thought would be to see if it is possible to send the energy around bends and more complex boundaries, which is what we discuss in Chapter 6.

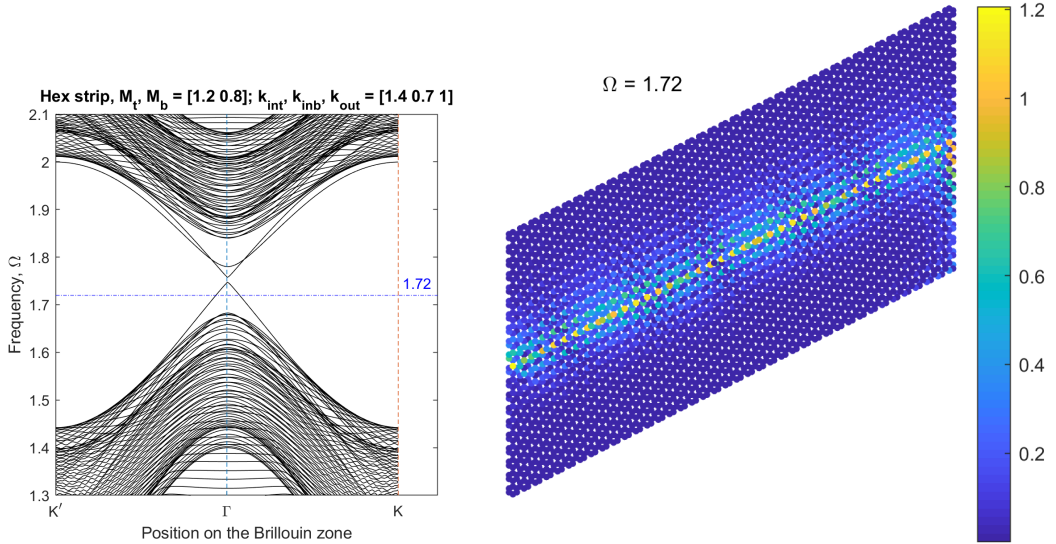


(a) Zoomed in look of Figure 4.9 near the bandgap. (b) The plot of $|y_i|$ for each mass in each cell.

Figure 5.4: Simulation of scattering on the hexagonal finite lattice in Figure 5.2 with the alternating masses as defined in Figure 4.9 with $\Omega = 1.6$.

5.2.2 Varying mass and stiffnesses

Now we take a look at running scattering simulations as above but for the physical system discussed in Chapter 4.3.2, which results in Figure 5.5.



(a) Zoomed in look of Figure 4.10 near the bandgap. (b) The plot of $|y_i|$ for each mass in each cell.

Figure 5.5: Simulation of scattering on the hexagonal finite lattice in Figure 5.2 with the top having a greater M and k than the bottom as defined in Figure 4.10 with $\Omega = 1.72$.

5.3 2d kagome finite lattice

Figure 5.6 shows a schematic view of the finite kagome lattice on which we will be running our scattering simulations. We will be exciting our lattice at the leftmost edge of the boundary. More specifically, we will have a positive excitation just above the boundary (at M_3), and a negative excitation just below the boundary (at M_3), i.e. \vec{F} is 0 everywhere except $\vec{F}_{3(\frac{N}{2}-1)+3} = 1$ and

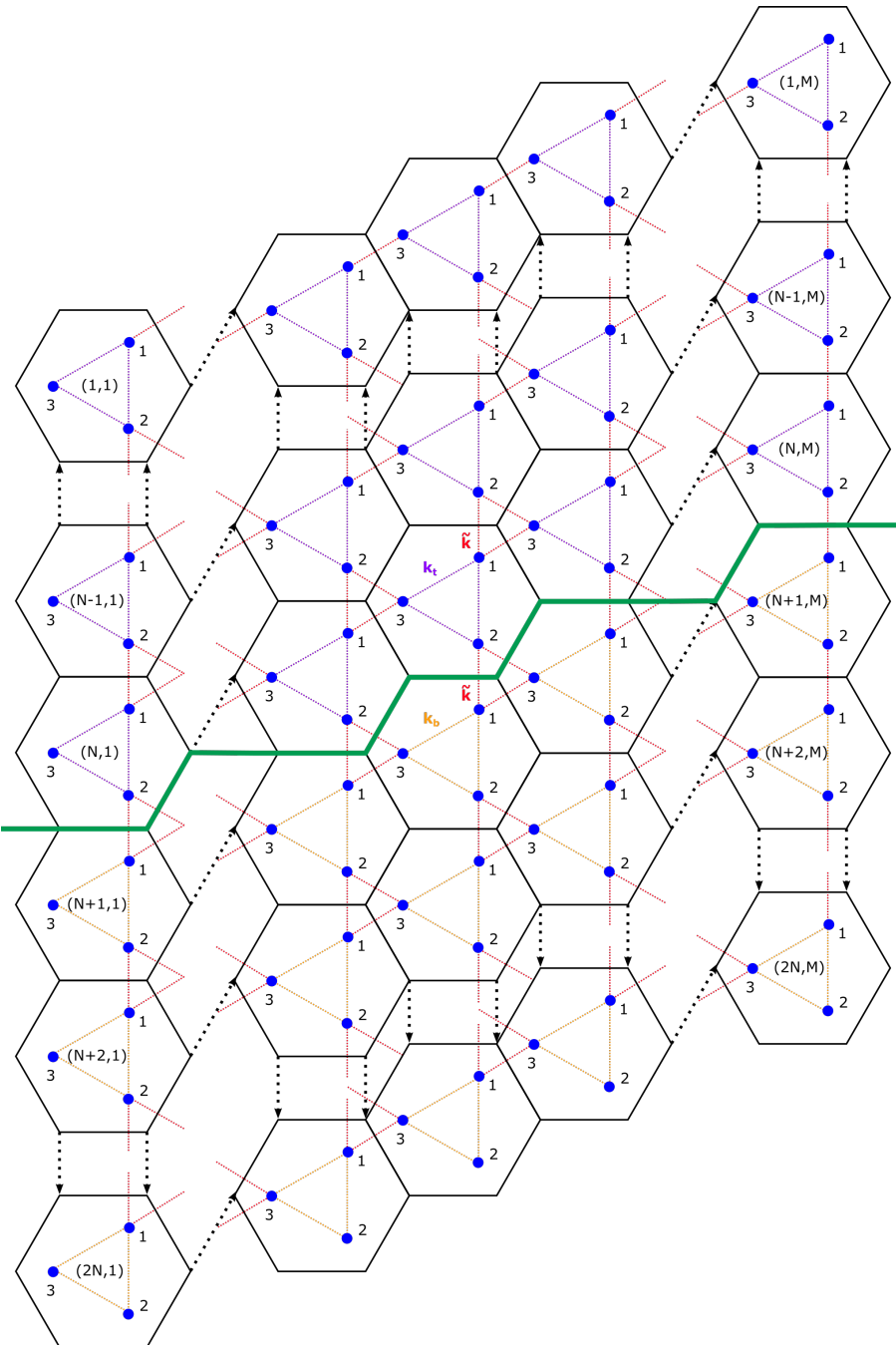


Figure 5.6: Schematic view of the finite kagome lattice formed from the joining of strips side-by-side, where the strips themselves are formed from two different halves as in Chapter 4. Note the conditions imposed at the boundaries (masses at boundaries have no connections outside the lattice).

$$\vec{F}_{3(\frac{N}{2})+3} = -1.$$

Running our simulation on the arrangement of cells in Figure 5.7, we get the edge state in Figure 5.8. The only difference between this and the hexagonal ones is that we can see there seems to be some of the energy being diverted down the right edge. This is due to the way we have set up the boundary conditions in which we have rigid boundaries. This boundary coinciding with the straight line connections of M_1 connected to M_2 allows certain waves to be transmitted along that boundary. Something very similar happens along the top boundary where there is a straight line connection between M_1 and M_3 , which we can see in Figure 6.1d.

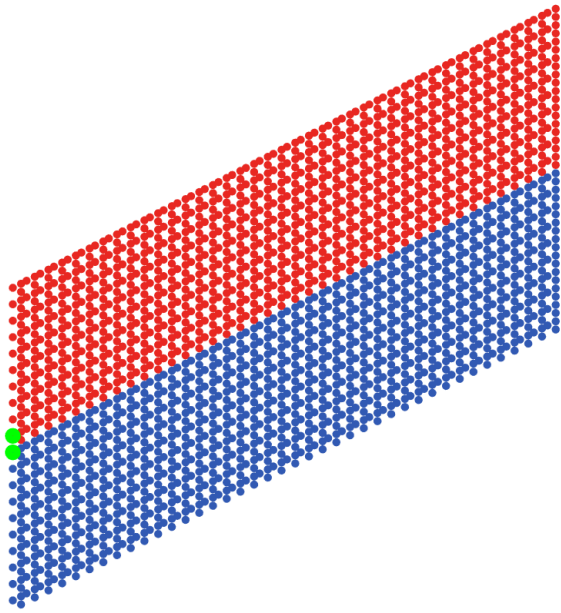


Figure 5.7: Arrangement of kagome cells ($2N = 20$, $M = 40$), with red and blue being different materials, and source of excitation at the green masses.

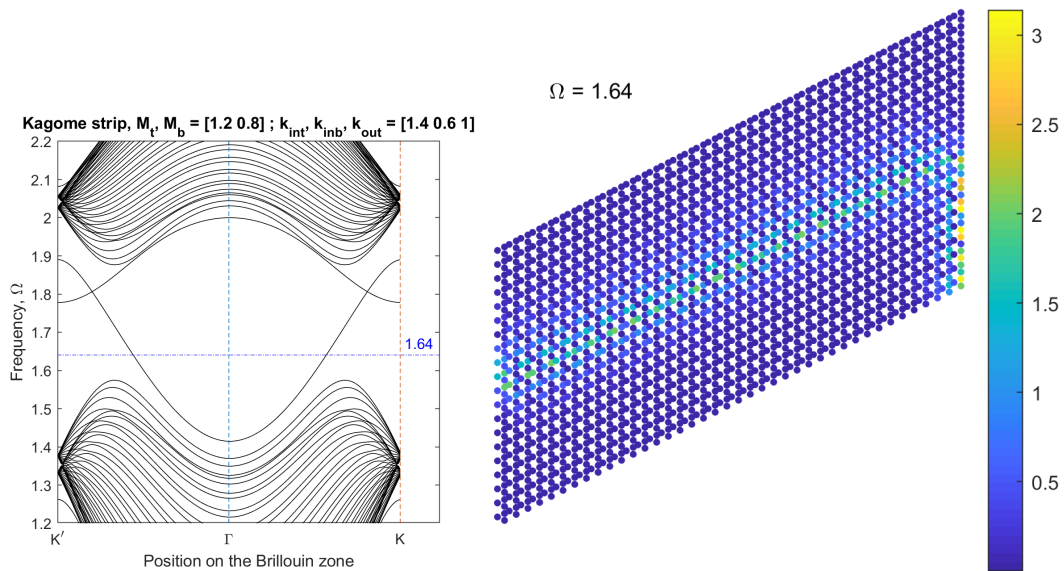


Figure 5.8: Simulation of scattering on the kagome finite lattice in Figure 5.7 with the top material with greater M and k than the bottom material as defined in Figure 4.16 with $\Omega = 1.64$.

Chapter 6

Complex bends

Now that we have built up the foundation of how we can force a wave to propagate in a specific direction in a topologically repeating material or metamaterial, we want to see just how robust this phenomenon is based on the shape of the boundary, i.e. just how much can we bend the wave?

Note: For the hexagonal simulations, we will specifically be using the same top and bottom cells as Figure 5.4, which is with alternating masses as defined in Figure 4.9. And for the kagome simulations, we will specifically be using the same top and bottom cells as Figure 5.8.

6.1 Gentle and sharp straight bends

So far we have seen just straight line boundaries, but can this work for bent boundaries too? Due to the way we set up our lattice (with the strips getting higher as we go from left to right), there are two kinds of bends we can make straight away. The 'gentle' bend where we bend the boundary upwards, and the 'sharp' bend where we bend the boundary downwards.

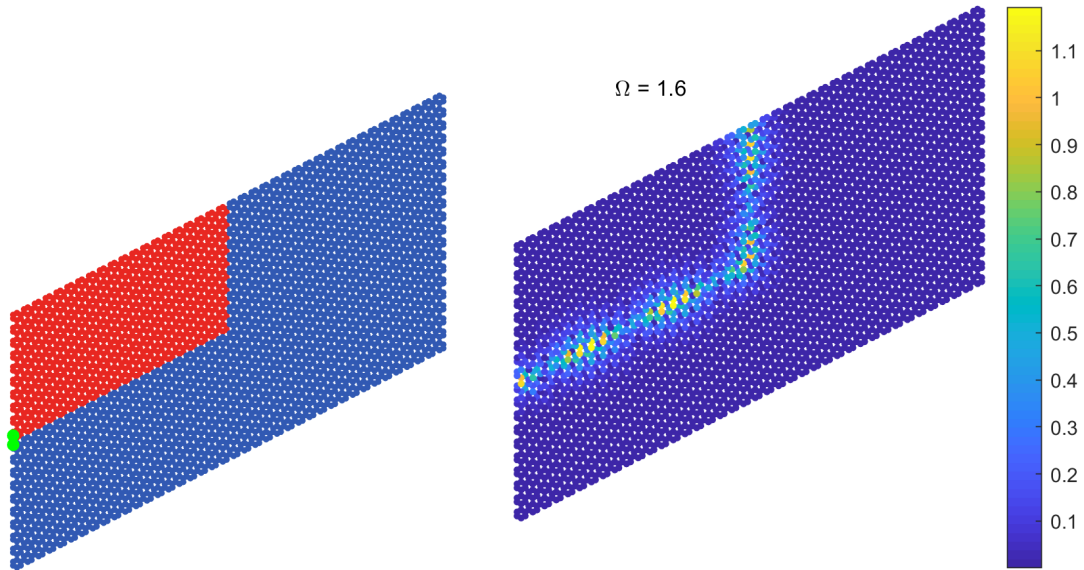
Amazingly, our systems are able to stand up to both of these bends as we can see in Figure 6.1 and Figure 6.2, and these type of bends may be useful in the production of lenses.⁸

6.2 Curved bends

So it can travel around gentle and sharp straight bends; it is only natural to then wonder if it can propagate as well along a curved bend. Being able to bend energy around a corner could be useful in the creation of an invisibility cloak.²

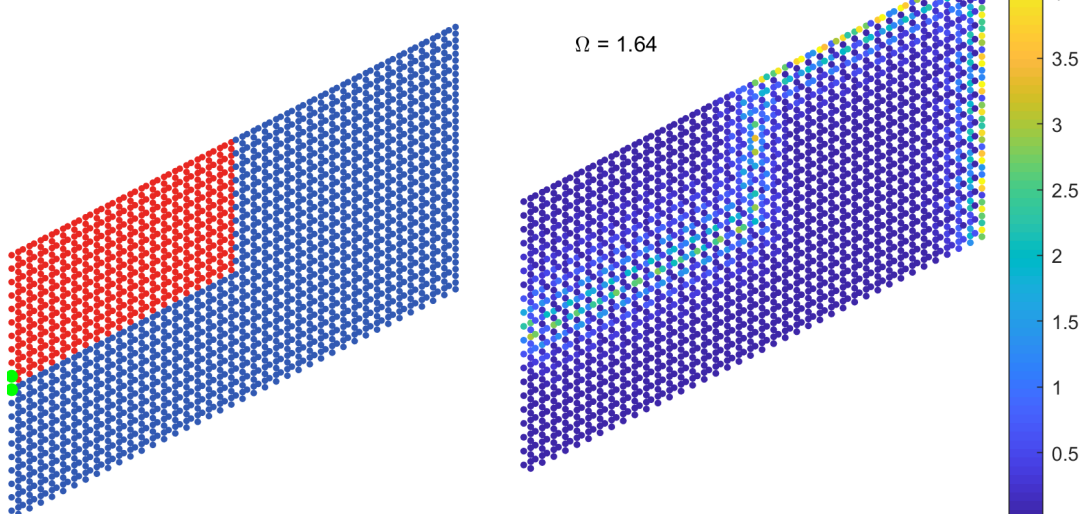
6.3 Energy splitting and merging

One of the applications of metamaterials that we have discussed is splitting and also focusing energy.^{3,4,7} And we see that we are able to get the energy splitting behaviour in Figure 6.4. Unfortunately we are unable to model the energy merging scenario in our system as we do not model the flow of energy over time, but just the overall steady state wave. However, we can imagine that we could have sources of excitation at the three branches and have them converge onto the single branch.



(a) Arrangement of cells to form a gentle bend.

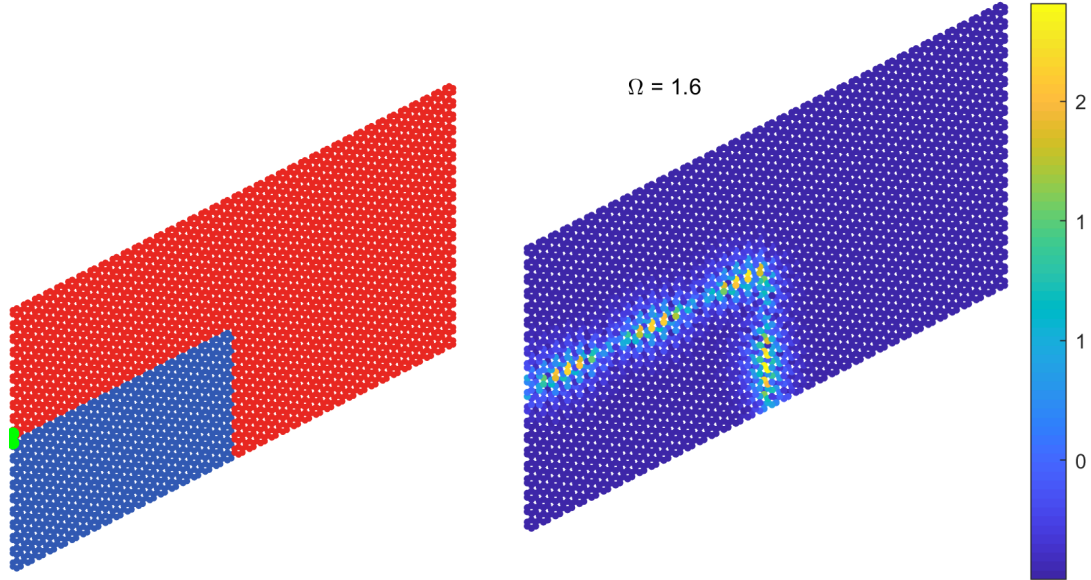
(b) The plot of $|y_i|$ for each mass in each cell.



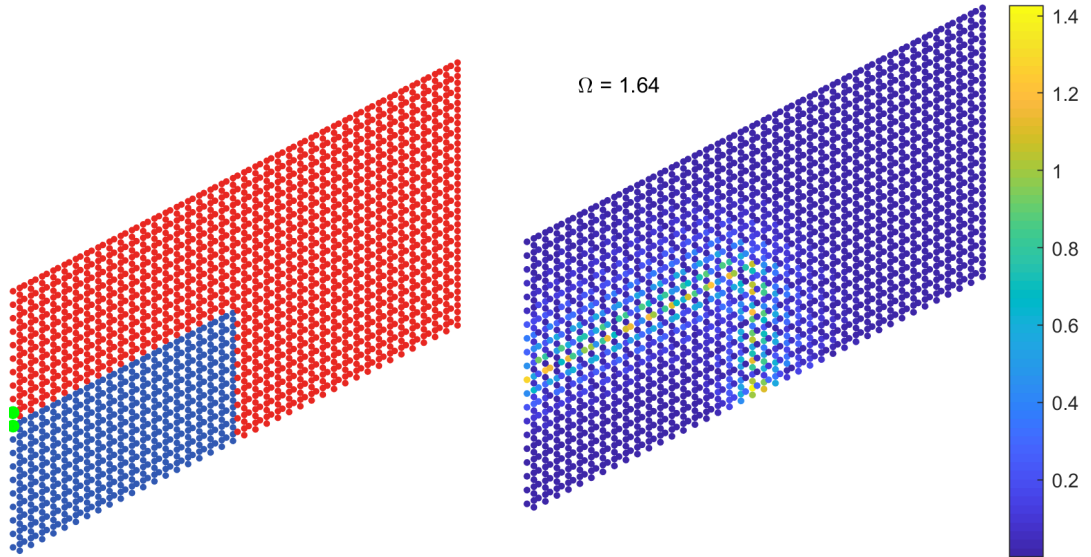
(c) Arrangement of cells to form a gentle bend.

(d) The plot of $|y_i|$ for each mass in each cell.

Figure 6.1: Simulation of scattering hexagonal and kagome finite lattices with a gentle bend.

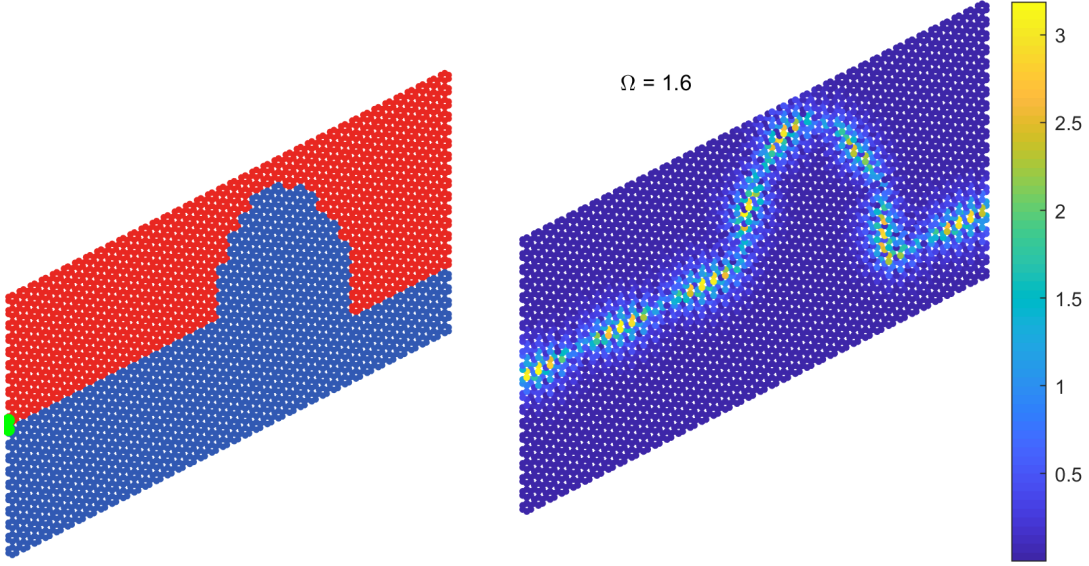


(a) Arrangement of cells to form a sharp bend. (b) The plot of $|y_i|$ for each mass in each cell. $\Omega = 1.6$



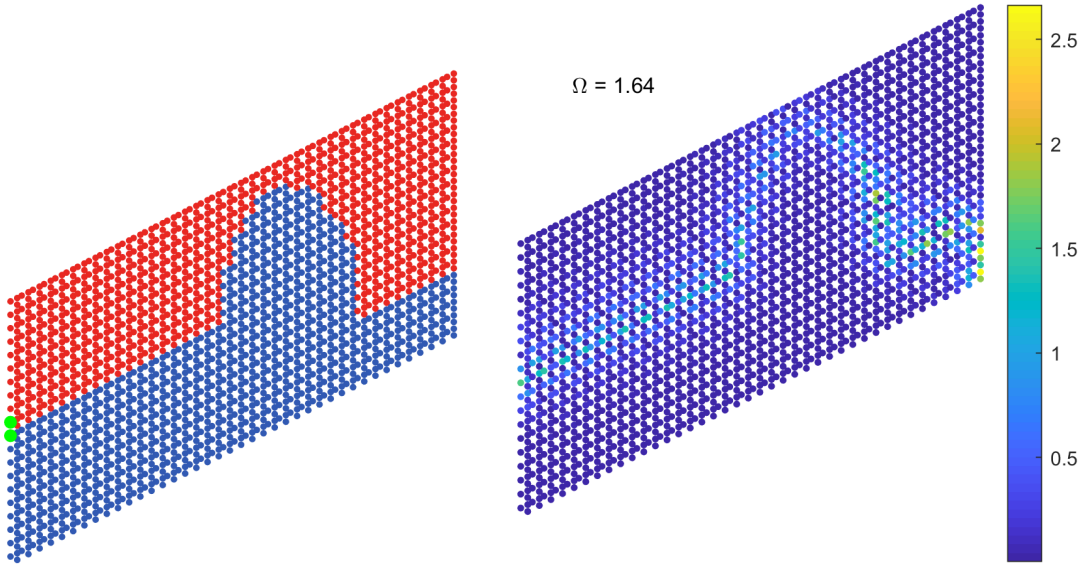
(c) Arrangement of cells to form a sharp bend. (d) The plot of $|y_i|$ for each mass in each cell. $\Omega = 1.64$

Figure 6.2: Simulation of scattering on the hexagonal and kagome finite lattice with a sharp bend.



(a) Arrangement of cells to form a curved bend.

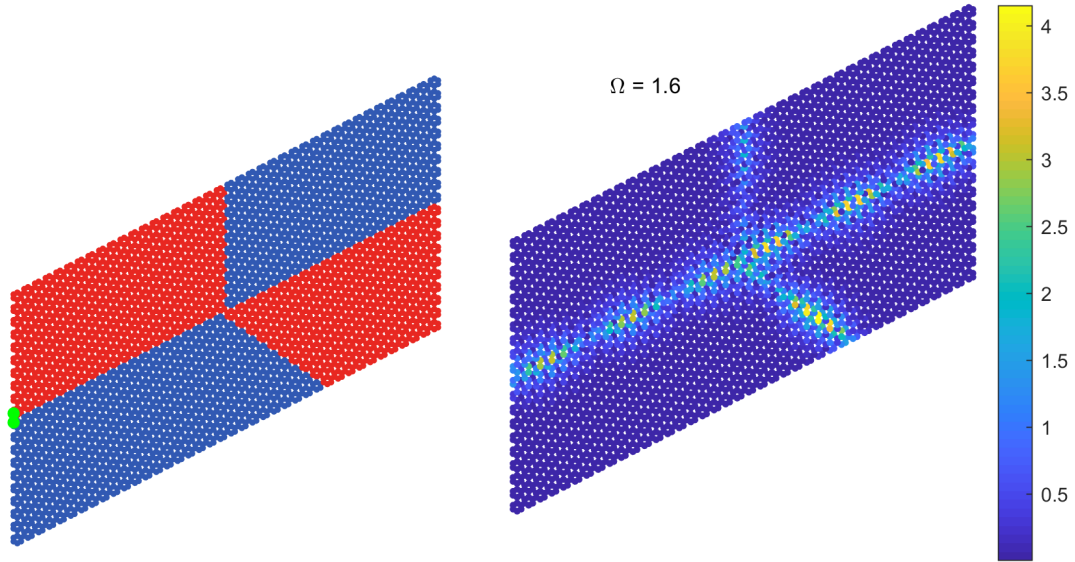
(b) The plot of $|y_i|$ for each mass in each cell.



(c) Arrangement of cells to form a curved bend.

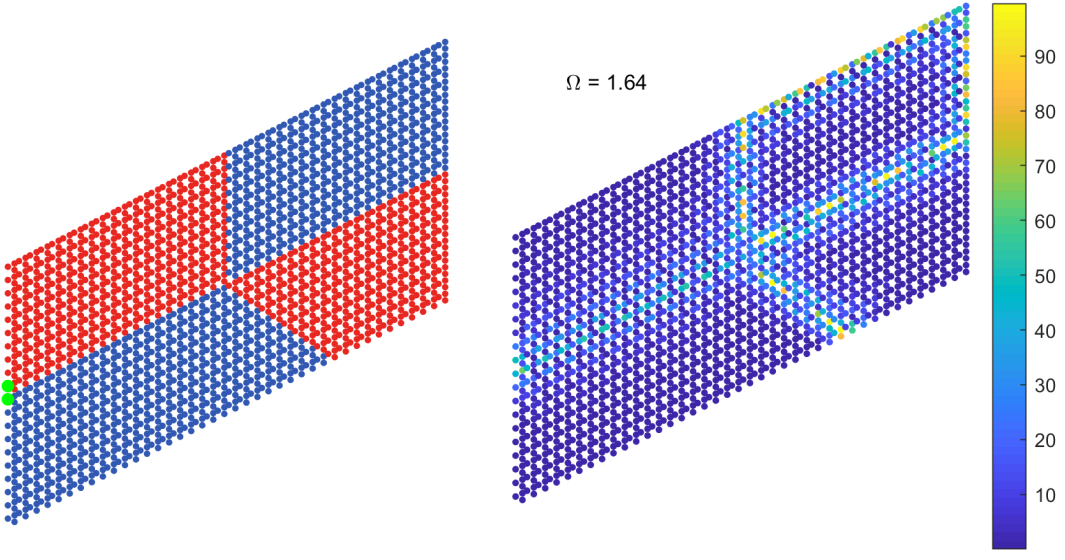
(d) The plot of $|y_i|$ for each mass in each cell.

Figure 6.3: Simulation of scattering on the hexagonal and kagome finite lattice with curved bend.



(a) Arrangement of cells to form a 3-way split.

(b) The plot of $|y_i|$ for each mass in each cell.



(c) Arrangement of cells to form a 3-way split.

(d) The plot of $|y_i|$ for each mass in each cell.

Figure 6.4: Simulation of scattering on the hexagonal and kagome finite lattice with a 3-way split, modelling a 3-way energy splitter.

Chapter 7

Evaluation

7.1 Reproducibility in other models

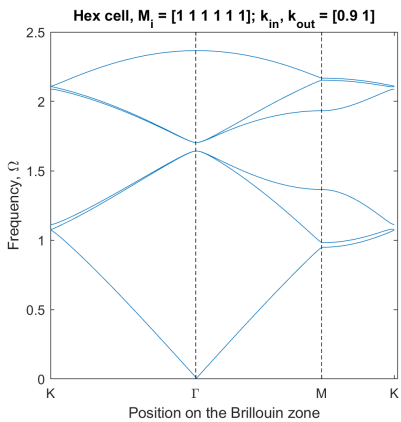
As mentioned in Chapter 2.2, most of the practical applications of metamaterials and photonic crystals come from their ability to control the propagation of acoustic or electromagnetic waves. As such, it is important to evaluate our model in terms of whether the results can translate to other complex models.

To evaluate the performance and accuracy of our mass-spring model, we will therefore compare our results to those produced in other papers. As we have used in one of our hexagonal lattice perturbations an analogue to the perturbation in this paper on photonic crystals,⁴³ we can try to recreate their results of band inversion to corroborate the validity and accuracy of our mass-spring model. In the paper, a band inversion take place upon reducing the lattice constant from just above 3 to just below 3 in their system. In our system, this corresponds to increasing the inner stiffness k from just above 1 to just below 1. We show that we do indeed get this band inversion in Figure 7.1.

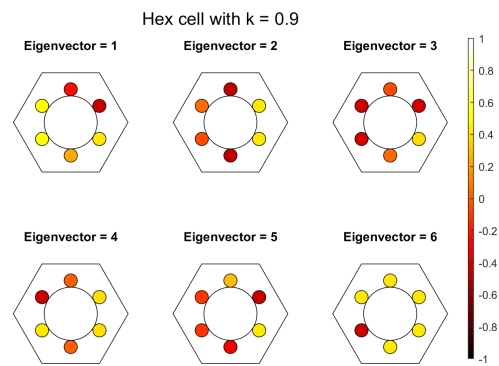
7.2 Extensibility and reusability of codebase

On the computing side of things, all our codes are written in Matlab. We chose to do so as it contains all the appropriate libraries to deal with matrices. Also at the same time we have tried to make it as reusable and extensible as possible. Some features that we have implemented

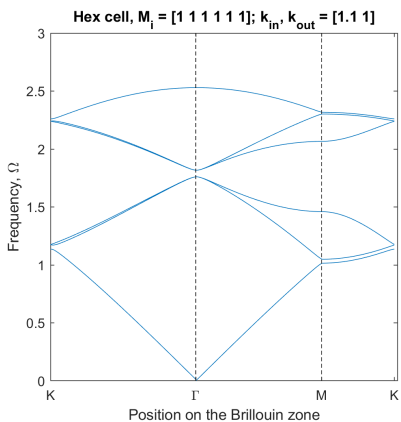
- Created generalised functions to form matrices \mathbf{A} and \mathbf{M} (such as in (4.4)) which takes the variable parameters of our systems as function parameters. This greatly increased the speed at which we are able to test out new systems with different configurations and ensured that the coupling terms are all in the correct places.
- For our scattering simulations in Chapter 5, we have implemented a system whereby we can input the arrangement of our cells in our lattice as a matrix of 0's and 1's, where 0 and 1 represent different materials. It will then generate the appropriate \mathbf{A} and \mathbf{M} for us, with all the coupling terms in the right positions. This greatly reduced the time it takes for us to generate scattering simulations for differing bends and curves. At the same time, it programmatically creates the matrix and outputs the schematic figure as well, so there is much less likelihood of there being a an error in, say, the position of a coupling term in our matrix than if we did each arrangement by hand (keep in mind that even for our hexagonal finite lattice which is only 20 cells tall and 40 cells wide, \mathbf{A} has size $4800 \times 4800!$). For example, we use the matrix



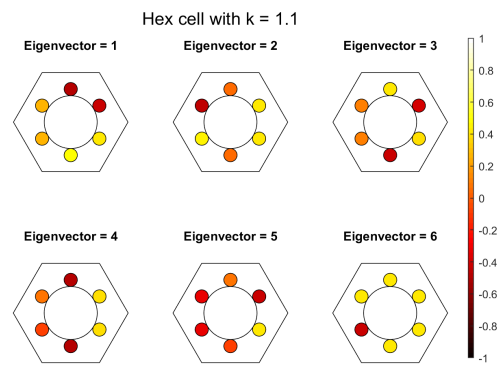
(a) Dispersion relation of hexagonal bulk lattice with $k = 0.9$, all other parameters set to 1.



(b) Visualisation of the six eigenvectors in each cell.



(c) Dispersion relation of hexagonal bulk lattice with $k = 1.1$, all other parameters set to 1.



(d) Visualisation of the six eigenvectors in each cell.

Figure 7.1: Band inversion for the hexagonal lattice when varying k from 0.9 to 1.1. Notice that eigenvectors 3 and 5 have swapped, and eigenvectors 2 and 4 have swapped.

$$\left[\begin{array}{cccccccccccccccc} \dots & 0 & 0 & 0 & 0 & 0 & 0 & 0 & 0 & 0 & 0 & 0 & 0 & 0 & 0 & 0 & 0 & \dots \\ \dots & 0 & 0 & 0 & 0 & 0 & 0 & 0 & 0 & 0 & 0 & 0 & 0 & 0 & 0 & 0 & 0 & \dots \\ \dots & 0 & 0 & 0 & 0 & 0 & 1 & 1 & 1 & 0 & 0 & 0 & 0 & 0 & 0 & 0 & 0 & \dots \\ \dots & 0 & 0 & 0 & 0 & 1 & 1 & 1 & 1 & 1 & 0 & 0 & 0 & 0 & 0 & 0 & 0 & \dots \\ \dots & 0 & 0 & 0 & 1 & 1 & 1 & 1 & 1 & 1 & 1 & 0 & 0 & 0 & 0 & 0 & 0 & \dots \\ \dots & 0 & 0 & 0 & 1 & 1 & 1 & 1 & 1 & 1 & 1 & 1 & 0 & 0 & 0 & 0 & 0 & \dots \\ \dots & 0 & 0 & 1 & 1 & 1 & 1 & 1 & 1 & 1 & 1 & 1 & 1 & 0 & 0 & 0 & 0 & \dots \\ \dots & 0 & 0 & 1 & 1 & 1 & 1 & 1 & 1 & 1 & 1 & 1 & 1 & 1 & 0 & 0 & 0 & \dots \\ \dots & 0 & 0 & 1 & 1 & 1 & 1 & 1 & 1 & 1 & 1 & 1 & 1 & 1 & 1 & 0 & 0 & \dots \\ \dots & 0 & 0 & 1 & 1 & 1 & 1 & 1 & 1 & 1 & 1 & 1 & 1 & 1 & 1 & 1 & 0 & \dots \\ \dots & 1 & 1 & 1 & 1 & 1 & 1 & 1 & 1 & 1 & 1 & 1 & 1 & 1 & 1 & 1 & 0 & \dots \\ \dots & 1 & 1 & 1 & 1 & 1 & 1 & 1 & 1 & 1 & 1 & 1 & 1 & 1 & 1 & 1 & 1 & \dots \\ \dots & 1 & 1 & 1 & 1 & 1 & 1 & 1 & 1 & 1 & 1 & 1 & 1 & 1 & 1 & 1 & 1 & 0 & \dots \\ \dots & 1 & 1 & 1 & 1 & 1 & 1 & 1 & 1 & 1 & 1 & 1 & 1 & 1 & 1 & 1 & 1 & 0 & \dots \\ \dots & 1 & 1 & 1 & 1 & 1 & 1 & 1 & 1 & 1 & 1 & 1 & 1 & 1 & 1 & 1 & 1 & 1 & \dots \\ \dots & 1 & 1 & 1 & 1 & 1 & 1 & 1 & 1 & 1 & 1 & 1 & 1 & 1 & 1 & 1 & 1 & 1 & \dots \\ \dots & 1 & 1 & 1 & 1 & 1 & 1 & 1 & 1 & 1 & 1 & 1 & 1 & 1 & 1 & 1 & 1 & 1 & \dots \\ \dots & 1 & 1 & 1 & 1 & 1 & 1 & 1 & 1 & 1 & 1 & 1 & 1 & 1 & 1 & 1 & 1 & 1 & \dots \\ \dots & 1 & 1 & 1 & 1 & 1 & 1 & 1 & 1 & 1 & 1 & 1 & 1 & 1 & 1 & 1 & 1 & 1 & \dots \\ \dots & 1 & 1 & 1 & 1 & 1 & 1 & 1 & 1 & 1 & 1 & 1 & 1 & 1 & 1 & 1 & 1 & 1 & \dots \\ \dots & 1 & 1 & 1 & 1 & 1 & 1 & 1 & 1 & 1 & 1 & 1 & 1 & 1 & 1 & 1 & 1 & 1 & \dots \\ \dots & 1 & 1 & 1 & 1 & 1 & 1 & 1 & 1 & 1 & 1 & 1 & 1 & 1 & 1 & 1 & 1 & 1 & \dots \\ \dots & 1 & 1 & 1 & 1 & 1 & 1 & 1 & 1 & 1 & 1 & 1 & 1 & 1 & 1 & 1 & 1 & 1 & \dots \end{array} \right] \quad (7.1)$$

to get the arrangement in Figure 6.3. From this, it can be seen that it helps the user a way to visually arrange the cells without having to bother about forming the right equations.

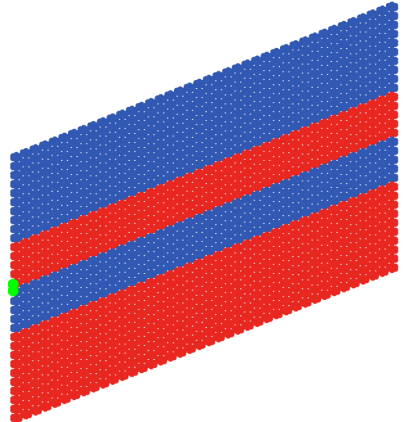
7.3 Further work

There are many things that we can improve on and continue investigating for the future.

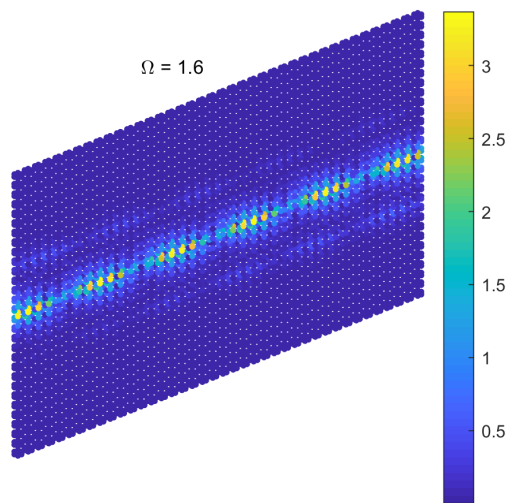
In terms of investigating deeper the challenges that might be faced when going from simulations to a real world product, the following could be useful:

- Evaluating the robustness of our system to imperfections in the lattice. This is crucial as real production systems have certain tolerances and are not perfect. As such, it is important to be able to test how little changes in the lattice can affect the edge states that we get, in terms of the strength of the energy which is transmitted as well as the amount of energy which is dissipated throughout the lattice.
- Testing how small each layer of material can be to get a *good enough* edge state. So far in our discussions of the strips of cells, we have been using strips with a large number of cells (e.g. $2N = 40$) because we know that the edge states decay exponentially outwards from the boundary, but this may not be possible or cost effective when developing real products. Therefore, it is important to study how the number of cells translates to the amount of energy lost and how this might lead to unwanted energy elsewhere in the system or interference with our edge state along the boundary. An example can be seen in Figure 7.2.
- Evaluating the difference in performance or robustness of the different types of perturbations used. In our work, we have seen two main ways of breaking the symmetry of our lattices and so inducing a topological valley-Hall effect. It would be useful to be able to characterise the differences and similarities which are present in these perturbed systems.
- Investigating the occurrence of resonance in our system. As we have chosen rigid boundary conditions, it is the case that we would get some resonance phenomenon when we have the frequency of the wave just right. This is what we see in Figure 6.4d where we can see that the magnitude of displacements are much greater than that of our other simulations. Also by perturbing the frequency by just a little, the magnitude of displacements falls back to within the range of our other simulations. As resonance in physical systems often lead to structural failures, it is important to be able to predict when it will occur.

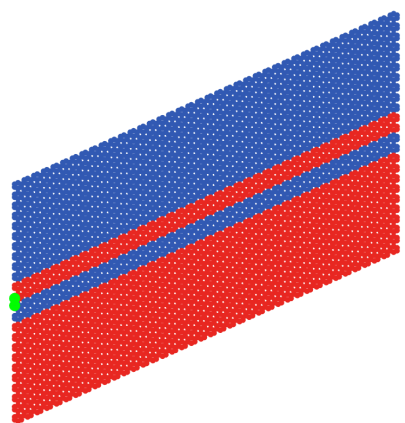
In terms of improving the workflow for the generation of these results for other geometries and topologies, we could implement the following:



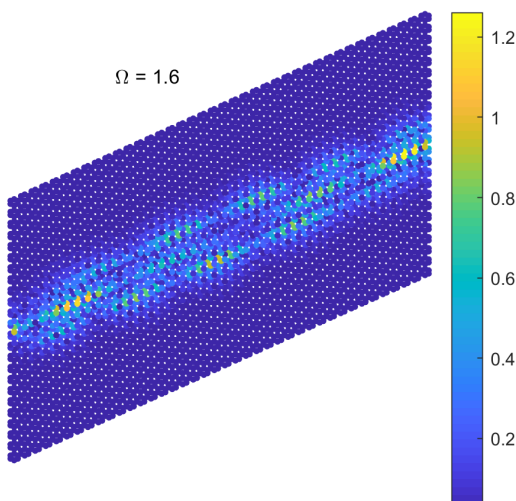
(a) Arrangement of cells with $2N = 10$.



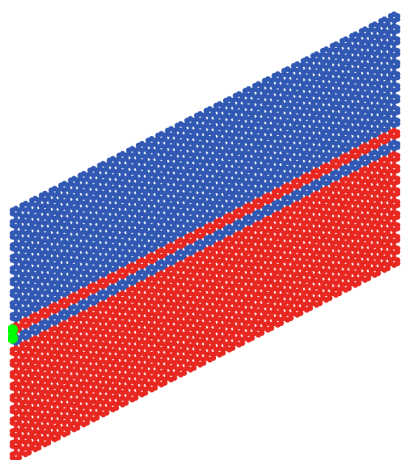
(b) The plot of $|y_i|$ for each mass in each cell.



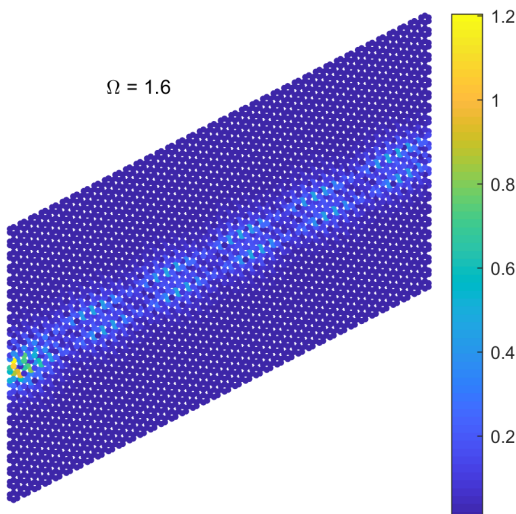
(c) Arrangement of cells with $2N = 4$.



(d) The plot of $|y_i|$ for each mass in each cell.



(e) Arrangement of cells with $2N = 2$.



(f) The plot of $|y_i|$ for each mass in each cell.

Figure 7.2: Scattering simulation to show the differences in amplitude and dissipation of energy for hexagonal boundaries of different thicknesses using the cells as defined in Figure 4.9.

- Move to an object-oriented programming model. We can implement the concepts of shapes and topologies as interfaces which contain information about the required geometries. Then we can create specific classes corresponding to actual shapes to extend those interfaces. We can then have our core code which generates the dispersion relations and scattering simulations work based on the interface implemented, rather than being specific to one shape class. This should be relatively straightforward to implement, as most of the code to solve for dispersion curves and scattering simulations is the same for any shape. The only big difference for different topologies is the formation of the eigen-problem matrix, which is a really mechanical but time-consuming procedure, and so this will make testing out new shapes or different connection of masses much easier.
- To take the above idea and make it even more user-friendly, we could create a graphical user interface where a user can choose things like the shape of the cell, the position of masses within the cell and how the masses are connected. This would allow faster and simpler prototyping of new designs.

Chapter 8

Conclusion

Herein we have constructed various different model mass-spring lattices on which we have built up not just the mathematics, but also the codes, to allow us to analyse the effects of different topological perturbations. This has led us to discovering various different configurations of lattices which permit a wide range of wave propagation manipulation. As we see that our results match those obtained from other models, we anticipate that our model system is a good approximation and can be used to model more complex waves. And from there, it is our hope that this powerful ability to manipulate and channel wave energy as we please can be used to further the good of humankind!

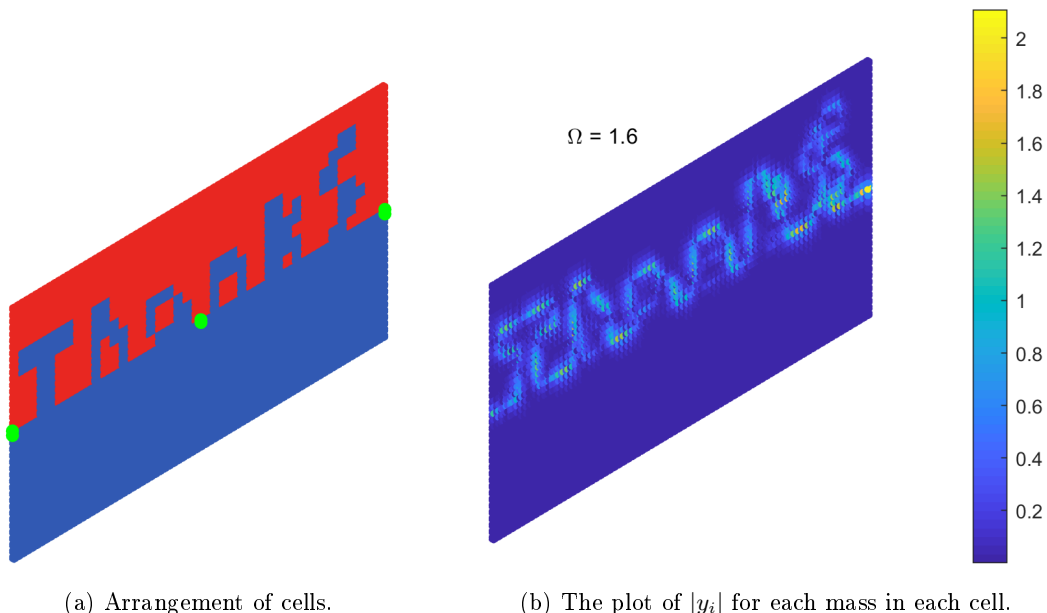


Figure 8.1: Simulation of scattering on the hexagonal finite lattice with the boundary spelling out a word commonly used in the English language to express gratitude.

Bibliography

- ¹ Carlton M. Caves. Quantum-mechanical radiation-pressure fluctuations in an interferometer. *Phys. Rev. Lett.*, 45:75–79, Jul 1980.
- ² D. Schurig, J. J. Mock, B. J. Justice, S. A. Cummer, J. B. Pendry, A. F. Starr, and D. R. Smith. Metamaterial electromagnetic cloak at microwave frequencies. *Science*, 314(5801):977–980, 2006.
- ³ Stefan Enoch, Gérard Tayeb, Pierre Sabouroux, Nicolas Guérin, and Patrick Vincent. A metamaterial for directive emission. *Phys. Rev. Lett.*, 89:213902, Nov 2002.
- ⁴ Vadym I Slyusar. Metamaterials on antenna solutions. 2009.
- ⁵ Hou-Tong Chen, Willie J Padilla, Joshua MO Zide, Arthur C Gossard, Antoinette J Taylor, and Richard D Averitt. Active terahertz metamaterial devices. *Nature*, 444(7119):597, 2006.
- ⁶ N I Landy, S Sajuyigbe, Jack J Mock, David R Smith, and Willie J Padilla. Perfect metamaterial absorber. *Physical review letters*, 100(20):207402, 2008.
- ⁷ Mehul P. Makwana and Richard V. Craster. Designing multidirectional energy splitters and topological valley supernetworks. *Phys. Rev. B*, 98:235125, Dec 2018.
- ⁸ J. B. Pendry. Negative refraction makes a perfect lens. *Phys. Rev. Lett.*, 85:3966–3969, Oct 2000.
- ⁹ Yafei Ren, Xinzhou Deng, Zhenhua Qiao, Changsheng Li, Jeil Jung, Changgan Zeng, Zhenyu Zhang, and Qian Niu. Single-valley engineering in graphene superlattices. *Phys. Rev. B*, 91:245415, Jun 2015.
- ¹⁰ C. L. Kane and E. J. Mele. Z_2 topological order and the quantum spin hall effect. *Phys. Rev. Lett.*, 95:146802, Sep 2005.
- ¹¹ Jiho Noh, Sheng Huang, Kevin P. Chen, and Mikael C. Rechtsman. Observation of photonic topological valley hall edge states. *Phys. Rev. Lett.*, 120:063902, Feb 2018.
- ¹² A. B. Khanikaev and G. Shvets. Two-dimensional topological photonics. *Nature Photonics*, 11:763–773, December 2017.
- ¹³ Tzuhsuan Ma and Gennady Shvets. All-si valley-hall photonic topological insulator. *New Journal of Physics*, 18(2):025012, feb 2016.
- ¹⁴ Xiao-Dong Chen, Fu-Li Zhao, Min Chen, and Jian-Wen Dong. Valley-contrasting physics in all-dielectric photonic crystals: Orbital angular momentum and topological propagation. *Phys. Rev. B*, 96:020202, Jul 2017.
- ¹⁵ J. Lu, C. Qiu, L. Ye, X. Fan, M. Ke, F. Zhang, and Z. Liu. Observation of topological valley transport of sound in sonic crystals. *Nature Physics*, 13:369–374, April 2017.
- ¹⁶ K. F. Mak, K. L. McGill, J. Park, and P. L. McEuen. The valley hall effect in mos2 transistors. *Science*, 344(6191):1489–1492, 2014.
- ¹⁷ Josh Bishop-Moser, Chris Spadaccini, and Christine Andres. Metamaterials manufacturing: Pathway to industrial competitiveness, April 2018.

- ¹⁸ Lord Rayleigh Sec. R.S. XXVI. On the remarkable phenomenon of crystalline reflexion described by Prof. Stokes. *The London, Edinburgh, and Dublin Philosophical Magazine and Journal of Science*, 26(160):256–265, 1888.
- ¹⁹ Eli Yablonovitch. Inhibited spontaneous emission in solid-state physics and electronics. *Phys. Rev. Lett.*, 58:2059–2062, May 1987.
- ²⁰ Sajeev John. Strong localization of photons in certain disordered dielectric superlattices. *Phys. Rev. Lett.*, 58:2486–2489, Jun 1987.
- ²¹ David Lindley. Focus: Landmarks—the birth of photonic crystals. *Physics*, 6:94, 2013.
- ²² Philip Russell. Photonic crystal fibers. *Science*, 299(5605):358–362, 2003.
- ²³ David Torres, Ori Weisberg, Gil Shapira, Charalambos Anastassiou, Burak Temelkuran, Max Shurgalin, Steven Alan Jacobs, Rokan U Ahmad, Tairan Wang, Uri Kolodny, et al. Omniduide photonic bandgap fibers for flexible delivery of co₂ laser energy for laryngeal and airway surgery. In *Photonic Therapeutics and Diagnostics*, volume 5686, pages 310–322. International Society for Optics and Photonics, 2005.
- ²⁴ Robert W. Ryan, Tamir Wolf, Robert F. Spetzler, Stephen W. Coons, Yoel Fink, and Mark C. Preul. Application of a flexible co₂ laser fiber for neurosurgery: laser-tissue interactions. *Journal of Neurosurgery JNS*, 112(2):434 – 443, 2010.
- ²⁵ R. S. Kshetrimayum. A brief intro to metamaterials. *IEEE Potentials*, 23(5):44–46, Dec 2005.
- ²⁶ Viktor G Veselago. The electrodynamics of substances with simultaneously negative values of ϵ and μ . *Soviet Physics Uspekhi*, 10(4):509–514, apr 1968.
- ²⁷ R. A. Shelby, D. R. Smith, and S. Schultz. Experimental verification of a negative index of refraction. *Science*, 292(5514):77–79, 2001.
- ²⁸ G.J. Chaplain, M.P. Makwana, and R.V. Craster. Rayleigh–bloch, topological edge and interface waves for structured elastic plates. *Wave Motion*, 86:162 – 174, 2019.
- ²⁹ Harish NS Krishnamoorthy, Zubin Jacob, Evgenii Narimanov, Ilona Kretzschmar, and Vinod M Menon. Topological transitions in metamaterials. *Science*, 336(6078):205–209, 2012.
- ³⁰ Raj Kumar Pal and Massimo Ruzzene. Edge waves in plates with resonators: an elastic analogue of the quantum valley hall effect. *New Journal of Physics*, 19(2):025001, feb 2017.
- ³¹ M. Miniaci, R. K. Pal, B. Morvan, and M. Ruzzene. Experimental observation of topologically protected helical edge modes in patterned elastic plates. *Phys. Rev. X*, 8:031074, Sep 2018.
- ³² Y. Shimazaki, M. Yamamoto, I. V. Borzenets, K. Watanabe, T. Taniguchi, and S. Tarucha. Generation and detection of pure valley current by electrically induced berry curvature in bi-layer graphene. *Nature Physics*, 11(12):1032–1036, nov 2015.
- ³³ R. Appleby and R. N. Anderton. Millimeter-wave and submillimeter-wave imaging for security and surveillance. *Proceedings of the IEEE*, 95(8):1683–1690, Aug 2007.
- ³⁴ D. Torrent, D. Mayou, and J. Sánchez-Dehesa. Elastic analogue of graphene: Dirac cones and edge states in the propagation of flexural waves in thin plates. In *2013 7th International Congress on Advanced Electromagnetic Materials in Microwaves and Optics*, pages 340–342, Sep. 2013.
- ³⁵ Karl F. Graff. *Wave motion in elastic solids*. Dover, 1991.
- ³⁶ L. D. Landau and Lifshitz E. M. *Theory of elasticity*. Elsevier, 2008.
- ³⁷ Jung-San Chen, Yi-Jyun Huang, and I-Ting Chien. Flexural wave propagation in metamaterial beams containing membrane-mass structures. *International Journal of Mechanical Sciences*, 131-132:500 – 506, 2017.
- ³⁸ Mehul P. Makwana and Richard V. Craster. Geometrically navigating topological plate modes around gentle and sharp bends. *Phys. Rev. B*, 98:184105, Nov 2018.

- ³⁹ Miguel C Junger and David Feit. *Sound, structures, and their interaction*, volume 225. MIT press Cambridge, MA, 1986.
- ⁴⁰ Yan Pennec, Jérôme O Vasseur, Bahram Djafari-Rouhani, Leonard Dobrzański, and Pierre A Deymier. Two-dimensional phononic crystals: Examples and applications. *Surface Science Reports*, 65(8):229–291, 2010.
- ⁴¹ J.C. Maxwell. On physical lines of force. *Philosophical Magazine*, 21, 23, 1861.
- ⁴² W. H. BRAGG. The reflection of x-rays by crystals. *Nature*, 91:477 EP –, Jun 1913.
- ⁴³ Long-Hua Wu and Xiao Hu. Scheme for achieving a topological photonic crystal by using dielectric material. *Phys. Rev. Lett.*, 114:223901, Jun 2015.
- ⁴⁴ Mehul P. Makwana and Richard V. Craster. Valley-hall states using network models for close-packed photonic crystals. Unpublished, forthcoming.
- ⁴⁵ Felix Bloch. Über die quantenmechanik der elektronen in kristallgittern. *Zeitschrift für Physik*, 52(7-8):555–600, 1929.
- ⁴⁶ Charles Kittel. *Introduction to Solid State Physics*, pages 167–168. Wiley, 8 edition, 2004.
- ⁴⁷ John D. Joannopoulos, Steven G. Johnson, Joshua N. Winn, and Robert David Meade. *Photonic Crystals: Molding the Flow of Light (second Edition)*, pages 233–238. 2011.
- ⁴⁸ Leon Brillouin. *Wave propagation in periodic structures; electric filters and crystal lattices, by Leon Brillouin*. McGraw-Hill Book Company New York, London, 1st ed. edition, 1946.
- ⁴⁹ Daniel Leykam, Alexei Andreeanov, and Sergej Flach. Artificial flat band systems: from lattice models to experiments. *Advances in Physics: X*, 3(1):1473052, 2018.